Assessing the effects of lanthanide-doped upconverting nanoparticles on the cellular homeostasis of healthy mammalian cells

Kais Bietar

Faculty of Medicine
Department of Physiology
McGill University, Montreal
December 2023

Supervisor: Dr. Ursula Stochaj

First Published on December 11, 2024

A Thesis Submitted to McGill University in Partial Fulfillment of

the Requirements of the Degree of Master of Science

Table of Contents

Abstract 4
Résumé 5
Acknowledgements 7
Contribution of authors 8
List of figures 9
List of Tables 10
List of abbreviations 10
1. Introduction 13
1.1. Nanoparticle types and modifications 13
1.2. Lanthanide-doped upconverting nanoparticles 16
1.3. Bio-nano interactions 18
1.4 Cytoskeletal organization 20
1.5. Oxidative stress response 21
1.6. Nucleolar stress 22
1.7. ER stress, the unfolded protein response and the proteostasis network 23
1.8. DNA damage 25
1.9. Nucleocytopalsmic shuttling 26
2. Aims and hypothesis 29
2.1. Effects of UCNPs on cellular homeostasis 32
2.2 Effects of UCNPs and their emissions on DNA damage and nuclear transport 32
3. Methods 33
3.1. UCNP synthesis and characterization 33
3.2. Cell culture 33
3.3. Cell seeding and treatment 33
3.3.1 Ln-UCNP treatment 33
3.3.2 Laser treatment 34
3.3.3. UV damage 34
3.4. Viability assay 35
3.5. Immunofluorescence staining and imaging 35
3.5.1 Fluorescence quantification 36
3.6. Western blotting 37
3.7 Statistical Analysis 37
4. Results 40
4.1. Ln-UCNPs are non-toxic and have minimal effects on stress biomarkers in mammalian cells. 40
4.1.1 Ln-UCNP characterization 40
4.1.2 Ln-UCNP cytotoxicity 42
4.1.3 Ln-UCNP uptake 46
4.1.4 Ln-UCNP effects on nuclear and cellular morphology 47
4.1.5 Ln-UCNP effects on oxidative stress and inflammatory markers 51
4.1.6 Ln-UCNP effects on nucleolar stress response 53
4.1.7. Ln-UCNP effects on ER stress response and molecular chaperones 55
4.2. Ln-UCNPs affect nucleocytoplasmic shuttling proteins in mammalian cells; their excitation has minimal effects on nucleic acid damage and other stress responses 57
4.2.1. Ln-UCNP emissions are non-cytotoxic 57

4.2.2 Ln-UCNP effects on nuclear import and export 61
5. Discussion 69
5.1. Ln-UCNPs have minimal cytotoxic effects after 24 hours 69
5.2. Ln-UCNPs have minimal, cell type specific, effects on cellular stress responses 69
5.3. Ln-UCNPs and their emissions do not affect DNA and RNA damage markers, and do not exacerbate observed Ln-UCNP effects on nucleocytoplasmic shuttling. 72
5.4. Future directions 72
Conclusion 74
References 75

Abstract

Lanthanide-doped upconverting nanoparticles (UCNPs) can absorb and convert low energy photons into higher energy photons in a process known as upconversion. UCNPs have unique physico-chemical properties that are ideal for biomedical and theranostics applications. When irradiated with near-infrared light, our UCNPs emit in the UV and visible part of the spectrum. To date, the use of UCNPs in living cells has been limited because of the poor understanding of their bio-nano interactions. To begin to fill this knowledge gap, our research focuses on the effects of $LiYF_4$ nanoparticles doped with the lanthanides thulium and ytterbium on nuclear homeostasis.

Cell toxicity, stress responses, proteostasis and cytoskeletal organization were evaluated in UCNP treated mouse fibroblasts (NIH3T3) and porcine kidney epithelial (LLC-PK1) cells. Moreover, nucleic acid damage and abnormalities in nucleocytoplasmic shuttling, as a result of near-infrared irradiation and subsequent UV emission by excited UCNPs, were evaluated through the analysis of DNA repair factors and RNA methylation, and major shuttling pathways. Viability and stress assays, quantitative immunofluorescence microscopy, and Western blot analyses were used to assess cell viability, morphology, and protein localization and abundance.

UCNP treatment for 24 hours, with and without irradiation, caused minimal changes on cell viability. Based on quantitative immunofluorescence microscopy and Western blotting, UCNPs had cell type specific effects on stress responses, proteostasis and cytoskeletal organization. Collectively, our experiments define the biocompatibility and subcellular interactions of UCNPs in non-malignant mammalian cells. Long-term, this research is expected to generate novel therapeutic and diagnostic tools that can be used for targeted drug delivery and biomedical imaging.

Résumé

Les nanoparticules à upconversion dopées aux lanthanides (UCNPs) peuvent absorber et convertir des photons à faible énergie en photons à énergie plus élevée dans un processus connu sous le nom d'upconversion. Les UCNPs présentent des propriétés physico-chimiques uniques qui sont idéales pour les applications biomédicales et théranostiques. Lorsqu'elles sont irradiées avec de la lumière proche infrarouge, nos UCNPs émettent dans le spectre UV et visible. Jusqu'à présent, l'utilisation des UCNPs dans les cellules vivantes a été limitée en raison de la méconnaissance de leurs interactions bio-nano. Pour commencer à combler cette lacune de connaissance, notre recherche se concentre sur les effets des nanoparticules de LiYF4 dopées aux lanthanides thulium et ytterbium sur l'homéostasie nucléaire.

La toxicité cellulaire, les réponses au stress, la protéostasie et l'organisation du cytosquelette ont été évaluées dans des fibroblastes de souris (NIH3T3) et des cellules épithéliales rénales de porc (LLC-PK1) traitées avec des UCNPs. De plus, les dommages aux acides nucléiques et les anomalies de la navette nucléocytoplasmique, résultant de l'irradiation proche infrarouge et de l'émission ultérieure d'UV par les UCNPs dopées en Ln excitées, ont été évalués par l'analyse des facteurs de réparation de l'ADN et de la méthylation de l'ARN, ainsi que des principales voies de navette. Des tests de viabilité et de stress, de la microscopie immunofluorescente quantitative et des analyses par Western blot ont été utilisés pour évaluer la viabilité cellulaire, la morphologie et la localisation et l'abondance des protéines.

Le traitement par les UCNPs pendant 24 heures, avec ou sans irradiation, a provoqué des changements minimes de la viabilité cellulaire. Sur la base de la microscopie immunofluorescente quantitative et de l'immunoprécipitation en Western blot, les UCNPs avaient des effets spécifiques aux types de cellules sur les réponses au stress, la protéostasie et

l'organisation du cytosquelette. Dans l'ensemble, nos expériences définissent la biocompatibilité et les interactions subcellulaires des UCNPs dans les cellules non malignes. À long terme, cette recherche devrait générer de nouveaux outils thérapeutiques et diagnostiques pouvant être utilisés pour la délivrance ciblée de médicaments et l'imagerie biomédicale.

Acknowledgements

I would like to express my sincere gratitude to everyone that contributed to the successful completion of my thesis. This journey would not have been possible without their unwavering support, guidance, and encouragement.

First and foremost, I would like to thank my supervisor, Dr. Ursula Stochaj. Your guidance and mentorship were invaluable throughout this research endeavor. I am truly grateful for the opportunities you've provided me.

I would also like to thank Siwei Chu, a PhD candidate in our lab, who was very generous with his time and efforts in training me and sharing his experiences to help me navigate through my research journey. I would also like to acknowledge the undergraduate students who contributed to the progress of my research: Renata Sabelli, Nay Najm, Vhaibhavii Shetty, Nikita Sharma, Jorge Galván Marroquín, Naim Chabytah and Emma Zhang.

Thank you to Dr. Gabrielle Mandl and Dr. John Capobianco who synthesized and characterized the nanoparticles, a fundamental aspect of my thesis. Your expertise and collaboration were indispensable in achieving our research objectives.

My heartfelt thanks go out to my committee members; Dr. Lisa Munter, Dr. Thomas Durcan and Dr. Susanne Bechstedt who evaluated my work, provided valuable feedback, and offered their insights. I very much appreciate your time and efforts.

Finally, I am grateful to my friends and family members for their unwavering support, understanding, and encouragement throughout this academic journey.

Contribution of authors

The experimental design for the results shared in this thesis was done by Dr. Ursula Stochaj and I. This thesis was written by me with input from Dr. Ursula Stochaj.

Nanoparticle synthesis and characterization was performed by Gabrielle Mandl, of Dr. John Capobianco's laboratory, at Concordia University. Cell culturing and treatment, viability assays, immunofluorescence quantification and the majority of immunofluorescence staining procedures were performed by me. Siwei Chu performed 24 hour viability assays on LLC-PK1 cells. Under my supervision, undergraduate students; Nay Najm, Renata Sabelli, Vhaibhavii Shetty, and Jorge Galván Marroquín performed some of the immunofluorescence procedures. Emma Zhang and Naim Chabaytah performed some immunofluorescence procedures on LLCPK1 cells, under Siwei Chu's supervision. All Western blots were performed by Dr. Ursula Stochaj. Data analysis and figures were done by Dr. Ursula Stochaj and I.

List of figures

Figure 1. Types of nanoparticles 15
Figure 2. Nanoparticle properties and surface modifications. 16
Figure 3. Theranostic UCNP 18
Figure 4. Subcellular bio-nano interactions 20
Figure 5. Nucleolar stressors and their consequences. 23
Figure 6. DNA repair mediated by H2AX 26
Figure 7. Nuclear import and export through the nuclear pore complex. 28
Figure 8. Main nuclear export pathways of RNAs. 28
Figure 9. Graphical representation of unfunctionalized-silica coated UCNPs and azide-functionalized silica-coated UCNPs. 30
Figure 10. Proof-of concept of AzSi-UCNPs conjugated to oligonucleotides. 31
Figure 11. UCNP Characterization. 41
Figure 12. UCNP 24-hour cytotoxicity assays. 44
Figure 13. UCNP three day and five day cytotoxicity assays. 45
Figure 14. UCNP uptake 46
Figure 15. UCNP effects on nuclear and cell morphology. 48
Figure 16. Effects of UCNPs on cell and nuclear area. 50
Figure 17. Effects of UCNPs on oxidative stress and inflammatory markers. 52
Figure 18. Effects of UCNPs on nucleolar stress markers. 54
Figure 19. Effects of UCNPs on ER stress markers and the proteostasis network. 56
Figure 20. UV effects on DNA damage markers. 58
Figure 21. Cytotoxic effects of UCNP emissions. 59
Figure 22. Effects of UCNPs and their emissions on DNA damage markers. 60
Figure 23. Effects of UCNPs and their emissions on RNA methylation. 61
Figure 24. Effects of UCNPs on nuclear export proteins. 63
Figure 25. Effects of UCNPs on importins and Ran. 64
Figure 26. Effects of UCNP emissions on nuclear export proteins. 66
Figure 27. Effects of UCNP emissions on importins and Ran. 68

List of Tables

Table 1. Immunofluorescence and Western blotting antibody dilutions related to results in section 4.1……..…….37

Table 2. Immunofluorescence antibody dilutions related to results in section 4.2……38

Table 3. Physical and chemical properties of UCNPs……...41

List of abbreviations

ATP: Adenosine triphosphate
ATF6: Activating trasncription factor 6
AU: Arbitrary units
AuNP: Gold Nanoparticle
AzSi-UCNP: Azide-functionalized silica coated upconverting nanoparticle
BCS: Bovine Calf Serum
BSA: Bovine serum albumin
CHOP: C/EBP homologous protein
cm: Centimeter
CRM1: Chromosome region maintenance 1 protein
DAPI: 4', 6-diamidino-2-phenylindole
ddH_2O: Sterile double-distilled water
DMEM: Dulbecco's modified eagle medium
DNA: Deoxyribonucleic acid
eIF2α: Eukaryotic translation initiation factor 2A
ER: Endoplasmic reticulum
ERAD: ER-associated degradation
Grp78: 78 kDa glucose-regulated protein [Also known as binding immunoglobulin protein (BiP)]
Grp94: 94 kDa glucose-regulated protein
GTP: Guanosine triphosphate
H2AX: H2A histone family member X
Hsp70: 70 kDa heat shock proteins

Hsp90: 90 kDa heat shock proteins

IF: Immunofluorescence

IRE1: Inositol requiring enzyme type 1

J: Joules

kD: Kilodaltons

KEAP1: Kelch-like ECH-associated protein 1

LLC-PK1: Porcine kidney epithelial cells

mL: Milliliter

mRNA: Messenger RNA

mV: millivolt

mW: Milliwatt

NES: Nuclear export signal

NF- κB: Nuclear factor-κB

NIH3T3: Mouse embryonic fibroblasts

NIR: Near-infrared

NLS: nuclear localization signal

nm: nanometer

NP: Nanoparticle

Nrf2: Nuclear factor erythroid 2-related factor 2

Nxf1: Nuclear RNA export factor 1

Nxt1: Nuclear transport factor 2- related export protein 1

PBS: Phosphate buffer saline

PDT: photodynamic therapy

PEG: Polyethylene glycol

PEN/STREP: Penicillin-Streptomycin

PERK: Protein kinase R-like endoplasmic reticulum kinase

PTT: photothermal therapy

Ran: Ras-related nuclear protein

RanGAP1: Ran GTPase-activating protein 1

RanGDP: Ran-guanosine diphosphate

RanGTP: Ran-Guanosine triphosphate

rDNA: Ribosomal DNA

RNA: Ribonucleic acid

rpm: Revolutions per minute

rRNA: Ribosomal RNA

SEM: Standard error of the mean

Si-UCNP: Unfunctionalized silica coated upconverting nanoparticle

TEM: Transmission electron microscopy

Tm^{3+}: Thulium

UCNPs: Upconverting nanoparticles

UPR: Untranslated protein response

UV: Ultraviolet

VCP: Valosin-containing protein

XPO1: Exportin-1

Yb^{3+}: Ytterbium

µg: Microgram

µm: Micrometer

ZO-1: Zonula Occludens-1

1. Introduction

Over the past few decades, nanotechnology has rapidly developed as an emerging tool in several industries including food, agriculture and medicine[1]. In medicine, several diseases require novel interventions as their current treatments are associated with poor therapeutic outcomes and poor patient quality of life. Many types of cancers, amyloidosis and fibrosis are a few examples of diseases that can benefit from novel diagnostic and therapeutic interventions[2–6]. The different variations and distinctive properties of nanoparticles allow them to be used as diagnostic and therapeutic agents which have the potential to aid in overcoming the challenges faced by current medical practices. There are currently clinically approved nanoparticle based therapies with promising patient outcomes. Thus, research on nanoparticle development has been gaining increased attention[7–9].

1.1. Nanoparticle types and modifications

Nanoparticles are characterized as materials measuring between 1-100 nm in diameter[10–12]. There are several types of nanoparticles (Figure 1) each with unique characteristics that are relevant for health applications[13]. These characteristics include their small size, high surface-area- to-volume ratio, reactivity to stimuli, ability to cross biological barriers and high stability in biological environments[14]. Moreover, nanoparticles can be precisely engineered to demonstrate desirable properties such as increased bioavailability and biocompatibility. This can be achieved by modification of the nanoparticle surface with targeting ligands and protective coatings to circumvent biological barriers and reduce toxicity and inflammatory reactions[1,12] (Figure 2).

As introduced, there are multiple different types of nanoparticles. Namely, nanoparticles are classified into organic NPs, inorganic NPs or hybrid/composite NPs[13,15,16]. Unlike organic nanoparticles, inorganic NPs exhibit excellent stability, making them suitable for long-term

applications by withstanding harsh environments. Inorganic NPs represent a versatile class of materials with unique properties for diverse applications[17]. Inorganic NPs are typically composed of metal NPs (e.g., gold, silver, and platinum), metal oxide NPs (e.g., titanium dioxide, iron oxide), or other inorganic compounds (e.g., semiconductor quantum dots) allowing for precise control over their size, shape, and surface properties[15].

One key advantage of inorganic NPs is their tunable surface chemistry. Various surface modifications, such as functionalization with organic ligands (eg. antibodies, azides) or polymers (carbohydrates), for targeting specific tissues or carrying drugs, enable the customization of their properties for specific applications[17–19]. Surface modifications, such as coating (PEGylation) of the NPs, also enhance the biocompatibility of inorganic NPs, facilitating their use in biomedical applications such as drug delivery and imaging. Moreover, inorganic nanoparticles can be modified to respond to internal or external stimuli, by doping with materials having optical or magnetic properties[19–21].

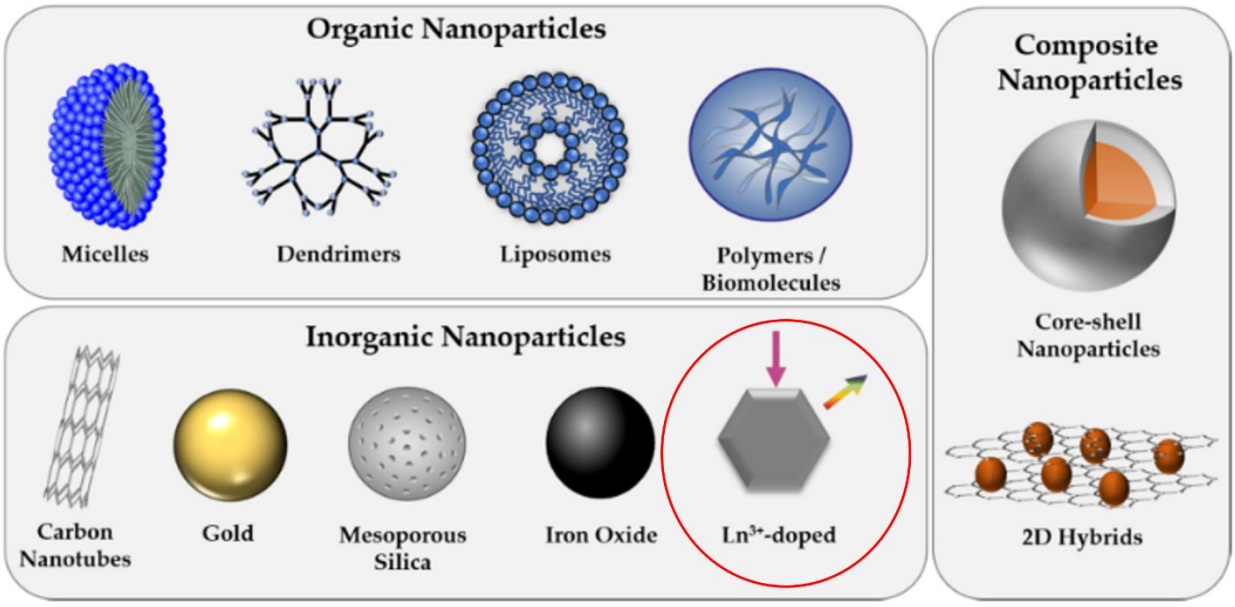

Figure 1. Types of nanoparticles. Adapted from Gessner and Neundorf (2020)[16].

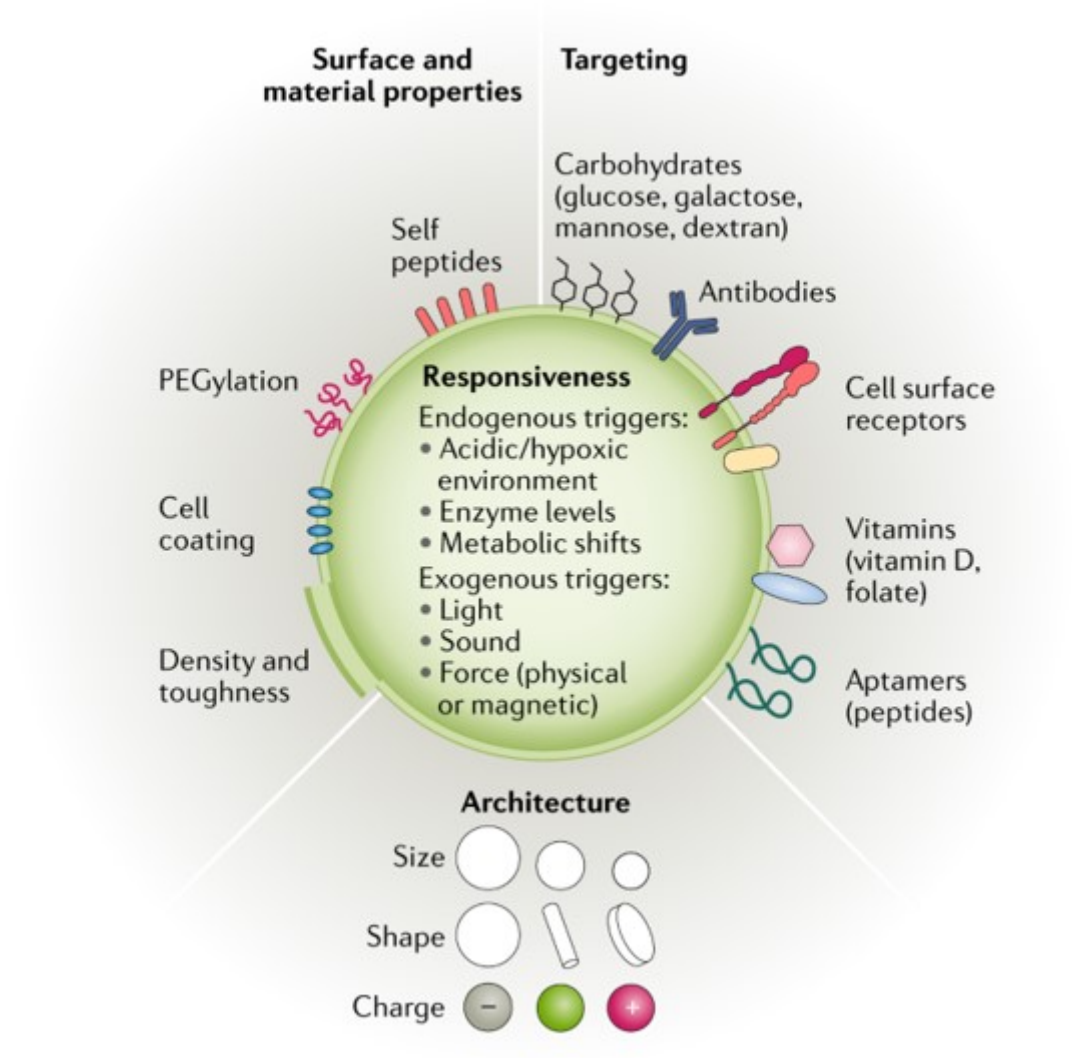

Figure 2. Nanoparticle properties and surface modifications. Adapted from Mitchell et al. (2020) with permission[12].

1.2. Lanthanide-doped upconverting nanoparticles

Luminescent materials respond to various energy stimuli, including, heat, chemical, mechanical and photon excitation converting that energy into light radiations[22]. Upconversion is an anti-stokes type emission where two or more photons of lower energy are sequentially absorbed, and a photon of higher energy is emitted[21,23]. Lanthanides are periodic table elements possessing these unique upconversion emission properties[22]. As a result, doping of nanoparticles

with lanthanides has gained increased interest. The resistance to photobleaching and photoblinking, low toxicity, high chemical stability, large anti-stokes shifts, and narrow emission bands of lanthanide-doped upconverting nanoparticles (UCNPs), relative to current photoluminescent particles, make them attractive candidates for biomedical applications[23]. These UCNPs absorb low energy near-infrared light, and emit higher energy NIR and UV or visible light[20,21,23]. Current treatments use photo stimulation or radiation for temporal and spatial control of molecules. Excitation of organic dyes, photosensitizers, photothermal agents, or photocleavable molecules is required for biodiagnostics, photothermal therapy (PTT), photodynamic therapy (PDT), or gene/drug delivery[5,21,24–26]. This is limited by the poor tissue depth penetration of UV light. UCNPs solve this problem as they absorb NIR light, which has good tissue depth penetration and is non-cytotoxic, then converts it to UV or visible light allowing for the activation of these photosensitizers, or breaking the bonds with photocleavable bioconjugates (Figure 3). Potentially minimizing the side effects of UV exposure and gaining higher efficiency[23].

It has been shown that lanthanide emissions are significantly more efficient in host lattices for UV emissions[22]. Moreover, the properties and emission intensities can be tuned by optimizing the size, shape, surface ligands, core/shell structure and emitters, and the dopant concentrations enabling the control of the emissions, biocompatibility and cellular uptake of the nanoparticles[23,27]. Extensive research demonstrated the increased efficiency of energy transfer upconversion, wherein, a NIR-absorbing sensitizer ion (Yb^{3+} or Nd^{3+}) and an emissive activator ion (Gd^{3+} or Tm^{3+}) are used. Also established, is the use of fluoride-based UCNPs, as they exhibit excellent chemical stability, do not photobleach or photoblink, have low-phonon energies and exhibit minimal cytotoxicity. This renders fluoride-based UCNPs ideal for biomedical

applications. A considerable amount of data is available for $NaYF_4$ core UCNP properties and biological interactions. However, $LiYF_4$ is a commonly overlooked material with excellent properties. $LiYF_4$ facilitates stronger upconversion in the UV when compared to $NaYF_4$. The different shapes of the bipyramidal $LiYF_4$ and spherical $NaYF_4$ particles could prove to have substantial differences in biological environments[27,28].

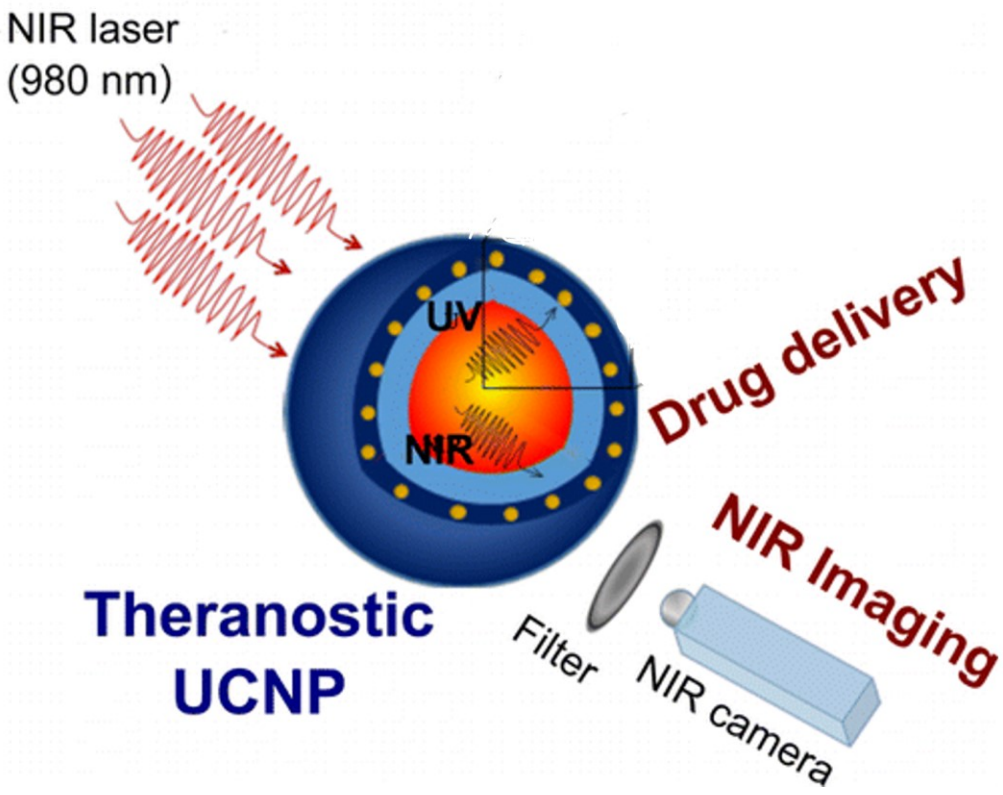

Figure 3. Theranostic UCNP. Adapted from Jalani et al. (2015)[29]. Image was modified. "This is an unofficial adaptation of an article that appeared in an ACS publication. ACS has not endorsed the content of this adaptation or the context of its use"

1.3. Bio-nano interactions

Introduction of nanoparticles to biological systems has several risks as their interactions with organs, tissues and cells is not clearly defined. There are multiple routes of administration for nanoparticles, majority of which lead to blood circulation[18]. Once in the blood, nanoparticles

are expected to be absorbed, distributed, metabolized (organic NPs) and excreted[30]. The biodistribution and bioavailability of nanoparticles is highly variable depending on size, shape and surface charge[18,30]. Nanoparticles smaller than ~10 nm are rapidly cleared from circulation when compared to 50 nm large nanoaprticles[10]. Modification of nanoparticle surface with protective coats could increase the blood circulation time. The barriers associated with delivery of nanoparticles, factors affecting their biodistribution and their excretion have been extensively reviewed by us and others[10,18,31]. Important for proper utility of nanoparticles, they need to interact with cells and be internalized. There are several methods of internalization for molecules, however the endocytic pathway has been shown to be mainly responsible for NP uptake. Specifically, clathrin-mediated and caveolin-mediated endocytosis[32,33]. Studies reported a significant decrease in NP association with cells upon specific inhibition of these endocytic pathways but not other pathways[33]. Again, shape, size and charge of NPs can also heavily affect the method and rate of uptake. NP internalization into cells could have major subcellular cytotoxic effects as NPs might interact with proteins, nucleic acids and lipids causing potential cytotoxic effects[34,35]. Steric hindrance is another factor resulting in cytotoxic effects as it can result in disruption of regular signaling and transport pathways. Several papers reported on the oxidative stress, ER stress, and nucleolar stress induced by NPs[36–41]. Figure 4 provides a schematic of the multiple factors affecting bio-nano interactions on the cellular level and the potential subcellular effects. Given the several factors affecting nanoparticle induced toxicity it is essential to define the subcellular interactions of nanoparticles both *in vitro* and *in vivo*. The currently accepted practice requires *in vitro* assays of cytotoxicity prior to *in vivo* experiments[42,43].

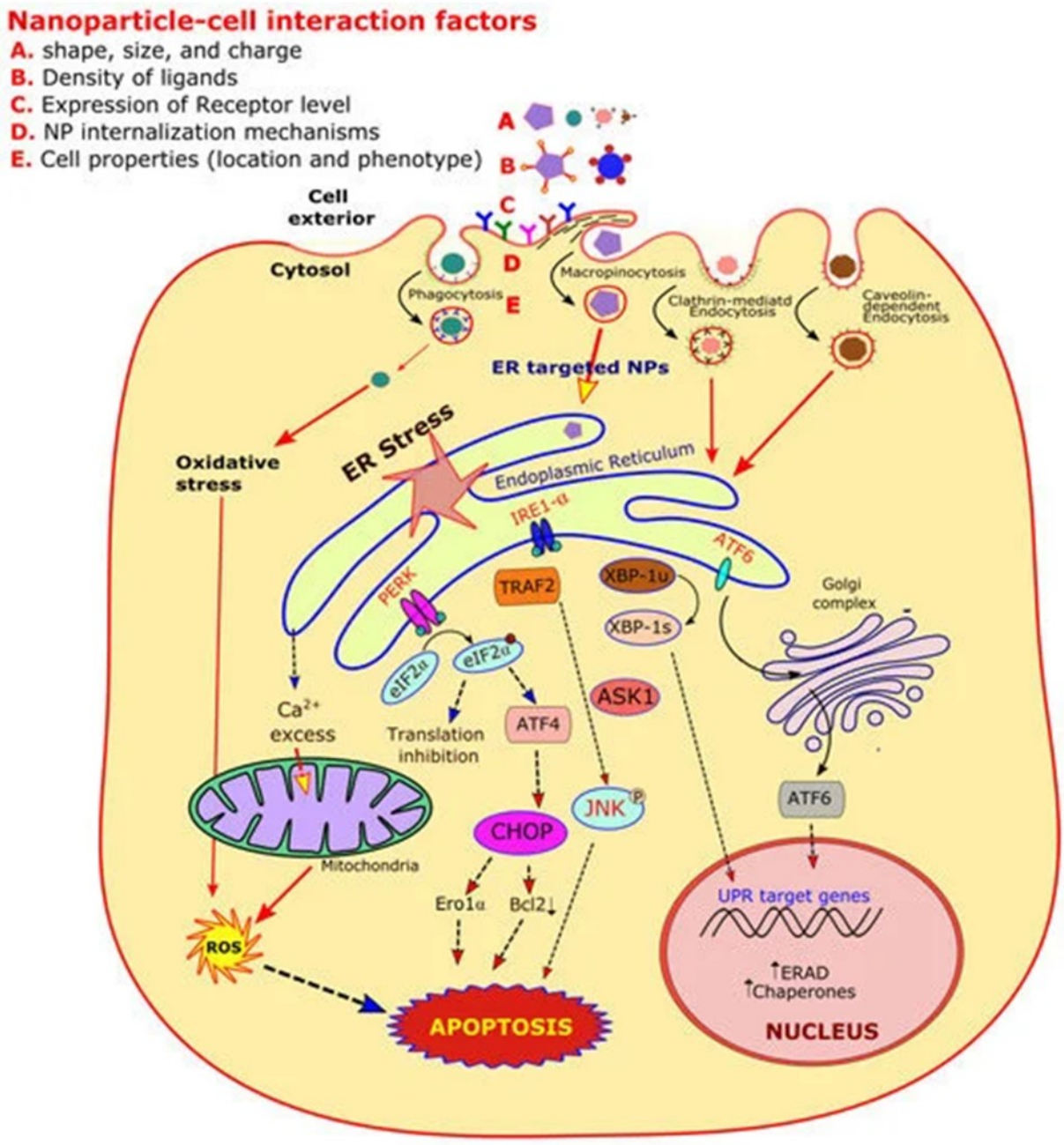

Figure 4. Subcellular bio-nano interactions. Adapted from Khan et al. (2020)[34].

1.4 Cytoskeletal organization

The cytoskeleton is a network of proteins responsible for maintenance of the structural integrity of the cell. Actin filaments, composed of actin polymers; microtubules, composed of α-tubulin and β-tubulin polymers; and intermediate filaments, make up the cytoskeletal network.[44]

Actin filaments and microtubules are dynamic structures which allows them to perform other functions. Besides their structural role, they also play major roles in cell movement, division and intracellular trafficking of endogenous or exogenous molecules. Moreover, cytoskeletal proteins are also involved in signal transduction and cross talks between the nucleus and the cytoplasm. Intermediate filaments, unlike actin filaments and microtubules, are less dynamic and are represented by a variety of proteins; they are expressed in multiple sites in the cell. Of particular importance, are lamins which are type V intermediate filament proteins responsible for the structural integrity of the nucleus. The nuclear lamina is closely associated with the nuclear envelope and is composed of lamins A, B1, B2 and C. Lamins are also closely linked to DNA repair processes[44–46]. Disruptions in the structural integrity and organization of cytoskeletal proteins is associated with impairments to multiple cellular processes including cell division, proliferation, intracellular transport and cell signalling. Moreover, stabilization of microtubules and downregulation of lamin B have been associated with cellular senescence[47,48].

As discussed in section 1.3., NPs are internalized into cells mainly by endocytic pathways. The formation of vesicles and their trafficking towards organelles can result in disruptions to the cytoskeletal organization. These changes are influenced by the physical properties of NPs such as shape, size or surface charge. Several papers report on the interactions of NPs with cytoskeletal proteins[49–51].

1.5. Oxidative stress response

The oxidative stress response is a tightly regulated process implemented by cells to withstand the overproduction of reactive oxygen species (ROS), such as superoxide anion (O_2^-), hydrogen peroxide (H_2O_2), hydroxyl radicals (OH^-), and singlet oxygen ($^1O_2$). ROS are normal byproducts of cellular metabolism that are metabolized by built in antioxidants. However, under

stress conditions like increased metabolic activity and UV exposure there is an overproduction of ROS, resulting in oxidative stress[52]. Increased activity of the transcription factors Nuclear factor erythroid 2-related factor 2 (Nrf2) and Nuclear factor-κB (NF- κB) is a hallmark of the oxidative stress response. Under physiological conditions, both proteins are sequestered in the cytoplasm by the constitutively active inhibitors KEAP1 and IkBα. When stressed, these transcription factors are released and translocate to the nucleus where they signal for the production of antioxidants, such as superoxide dismutase, catalase, and glutathione peroxidase, or the production of inflammatory cytokines[40,53]. However, both proteins are also susceptible to activation by other common stress pathways.[54–56] For example, NF-κB is also suggested to be constitutively active in response to downstream effects on nucleolar stress.[57]

1.6. Nucleolar stress

Ribosomes are integral to the survival of cells as they are responsible for the production of proteins from messenger RNA. Ribosome biogenesis is a tightly maintained, and highly energy consuming process in the cell. Hence, it is linked to metabolic and proliferative activity. The rate limiting step is ribosomal DNA (rDNA) transcription and processing which takes place in the subnuclear compartment known as the nucleolus. The nucleolus has a highly dynamic structure and is maintained by its function of pre-rRNA transcription, processing and assembly. These events occur in distinct subnucleolar compartents; namely, the fibrillar center, the dense fibrillar compartment and the granular compartment, respectively. The different subnucleolar compartments are marked by proteins involved in the distinct events leading to ribosomal biosynthesis. Disruption of cellular homeostasis by nutrient deprivation, exposure to cytotoxic agents, or oncogene inactivation leads to the downregulation of rDNA transcription and activation of nucleolar stress pathways, resulting in alterations in nucleolar size and morphology,

as well as, upregulation of p53 (Figure 5). p53 is a tumor suppressor protein that responds to various cell stressors as it is downstream of various cell stress signalling pathways. Processes affected by nucleolar stress include metabolism, cell cycle progression, autophagy, senescence, and apoptosis[58–61].

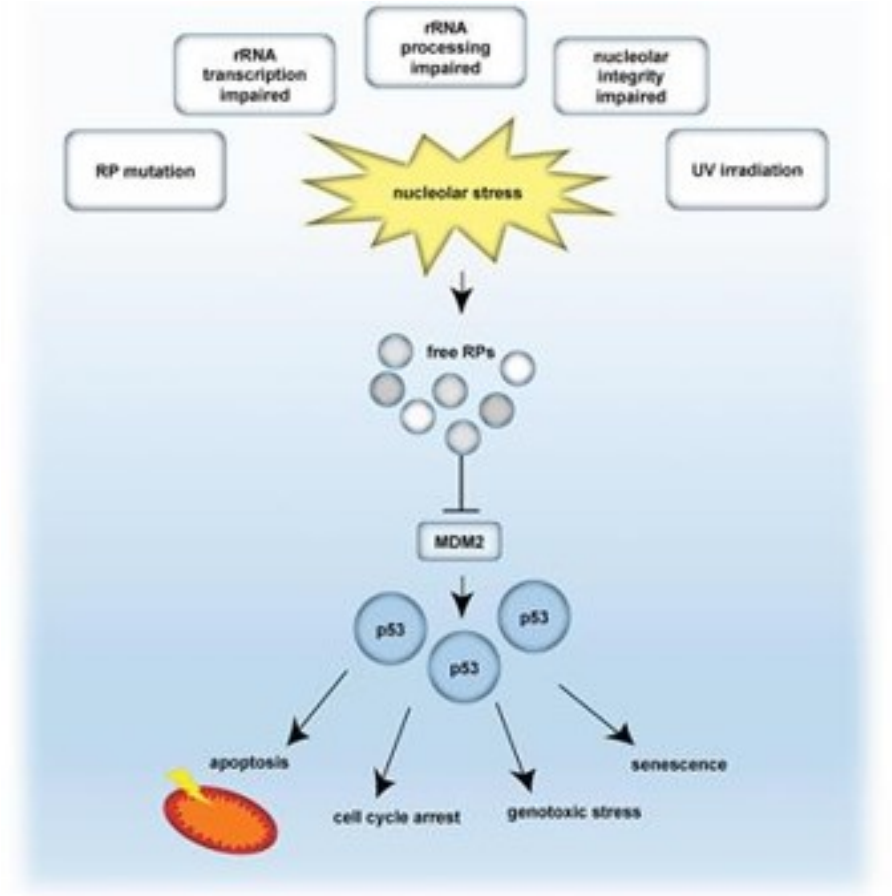

Figure 5. Nucleolar stressors and their consequences. Adapted from Pfister (2019)[60].

1.7. ER stress, the unfolded protein response and the proteostasis network

Proteostasis (protein homeostasis) refers to the maintenance of protein function, folding and degradation. This is mediated by molecular chaperones which aid in protein refolding and the ubiquitin proteasome system for targeted degradation of damaged proteins. Proteins produced by ribosomes require further processing to ensure proper function. Newly synthesized polypeptides are transported to the endoplasmic reticulum for proper folding into functional

conformations. To ensure production of properly folded functional proteins, this process is tightly regulated by built in quality control mechanisms that recognize misfolded or unfolded proteins[62,63]. The AAA-ATPase, valosin-containing protein (VCP), functions as a critical player in protein quality control by participating in ER-associated degradation (ERAD). Where VCP extracts misfolded proteins from the ER for subsequent degradation by the ubiquitin-proteasome system ensuring the clearance of unwanted or misfolded proteins[64].

ER stress occurs when misfolded or unfolded proteins accumulate. Which can be induced by several factors including oxidative stress, nutrient deprivation and impaired calcium regulation and the ER redox state. To re-establish ER homeostasis, the untranslated protein response (UPR) is activated. The UPR primarily involves three ER-resident transmembrane proteins, including IRE1, PERK, and ATF6, which, upon activation, initiate a cascade of events resulting in the upregulation of chaperones, such as GRP78 and GRP94, which facilitate protein folding and prevent protein aggregation. PERK activation, marked by phosphorylation of eif2α, results in global translation inhibition. Failure to alleviate ER stress leads to activation of pro-apoptotic pathways by upregulation of genes, such as CHOP. Hence, ER stress, the UPR and the proteostasis network are interconnected cellular mechanisms crucial for maintaining protein homeostasis and ensuring cell survival[62,63].

Moreover, ER-stress has been linked to activation of Nrf2 and NF-κB. It is suggested that Nrf2 is directly activated by PERK[55,56]. However, the mechanism of NF-κB activation is not fully understood. Oxidative protein folding in the ER, forms disulfide bonds and generates hydrogen peroxide (H_2O_2). Under stress conditions, disulfide bonds are dysregulated, and breakage may result in ROS production causing oxidative stress. Other factors, such as ER-stress

induced mitochondrial dysfunction and production of CHOP have also been linked to oxidative stress[65].

1.8. DNA damage

Nucleic acids are integral for the survival of cells as they make up the genetic code. Both DNA and RNA are susceptible to damage induced by endogenous and exogenous factors. Oxidative stress and UV exposure are major contributors to DNA damage. Base damage and modifications, DNA strand breaks, and the formation of thymine dimers in DNA induced by these stressors can result in disruption of DNA replication and transcription, leading to mutations in gene expression or inhibition of protein translation. As with other processes, cells have mechanisms to repair DNA damage; including base excision repair, nucleotide excision repair, and double-strand break repair. H2A histone family member X (H2AX) is a protein involved in the repair of DNA breaks. H2AX is present in chromatins, upon formation of DNA breaks, H2AX is phosphorylated forming γ-H2AX (Figure 6). γ-H2AX later recruits DNA repair proteins to the site of DNA breaks. Under chronic stress, H2AX dissociates from chromatins rendering the DNA site irreparable[66,67].

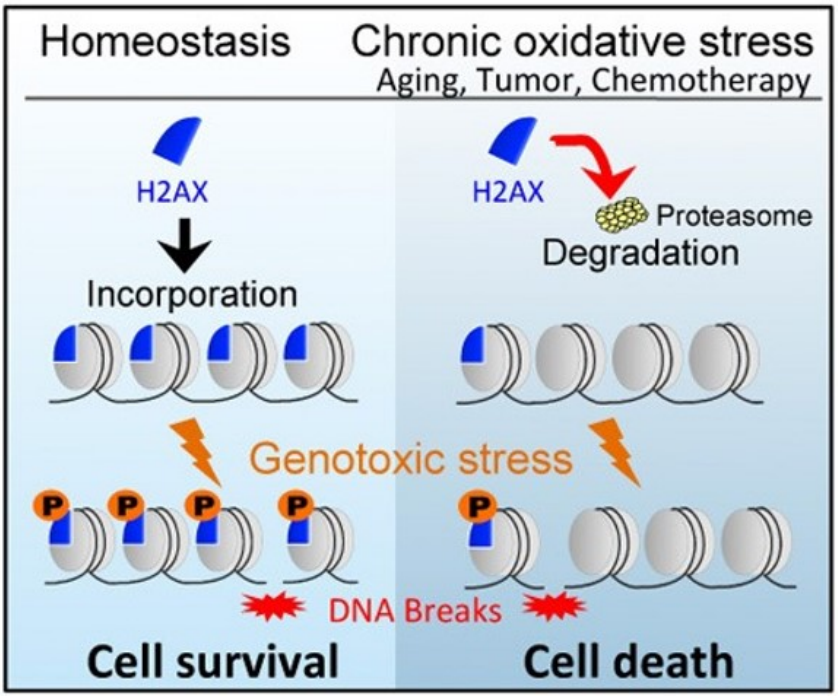

Figure 6. DNA repair mediated by H2AX. Adapted from Gruosso et al. (2016)[68].

1.9. Nucleocytopalsmic shuttling

Nuclear components are sheltered from the cytosol by the nuclear envelope. Communication between the nucleus and the cytoplasm is essential for the regulation of various cellular processes. For example, RNA transcription occurs in the nucleus by polymerases, whereas protein translation occurs in the Rough ER and cytoplasm by ribosomes[61,69]. Therefore, transport of RNAs to the cytoplasm and polymerases to the nucleus is essential for normal cell function. Molecules that need to be transported in or out of the cell pass through the nuclear pore complex (NPC), composed of proteins called nucleoporins. The passage of molecules through NPCs is tightly regulated. Molecules smaller than 10 nm in diameter can simply diffuse through the NPC. However, larger molecules, up to 40 nm in diameter, require transport carriers to pass through the NPC.

Nuclear import and export is mainly performed by members of the karyopherin family. Typically, importins recognize molecules with a nuclear localization signal (NLS) and exportins

recognize molecules with a nuclear export signal (NES). These processes are dependent on a class of proteins known as Ras-related nuclear protein (Ran). Nuclear import and export is mediated by the Ran gradient established by RanGTP and RanGDP levels in the nucleus and the cytoplasm, respectively (Figure 7). The major proteins that facilitate nuclear import are importin-α and importin-β. In the cytoplasm, these proteins form a complex with RanGDP and the cargo protein containing a NLS, transporting it across the nuclear envelope, through the nuclear pore complex. Phosphorylation of RanGDP to RanGTP in the nucleus results in disassembly of the complex and release of the cargo. Nuclear export is mediated by several different exportins. However, cargos containing a NES are mostly exported by Chromosome region maintenance 1 protein (CRM1), also known as Exportin-1 (XPO1). Similar to nuclear import, CRM1 forms a complex with cargos containing an NES, and RanGTP, transporting the cargo through the NPC into the cytoplasm, where RanGTP is dephosphorylated, disassembling the complex and releasing the cargo in the cytoplasm. Most proteins and RNAs are exported by transporters of the karyopherin family in a Ran-dependent form (Figure 8). One exception is mRNAs, which are transported in a Ran-independent fashion by the non-karyopherin member TAP/Nxf1 (Nuclear RNA export factor 1). Pre-processed mRNA forms a complex with Nxt1 (Nuclear transport factor 2-related export protein 1), transporting the mRNA through the NPC and releasing it in the cytoplasm by association with ATP rather than GTP. The process of nucleocytoplasmic transport is much more complex and is associated with multiple adaptors depending on the cargo transported. Comprehensive reviews detailing the intricacies of this process are available[69–72].

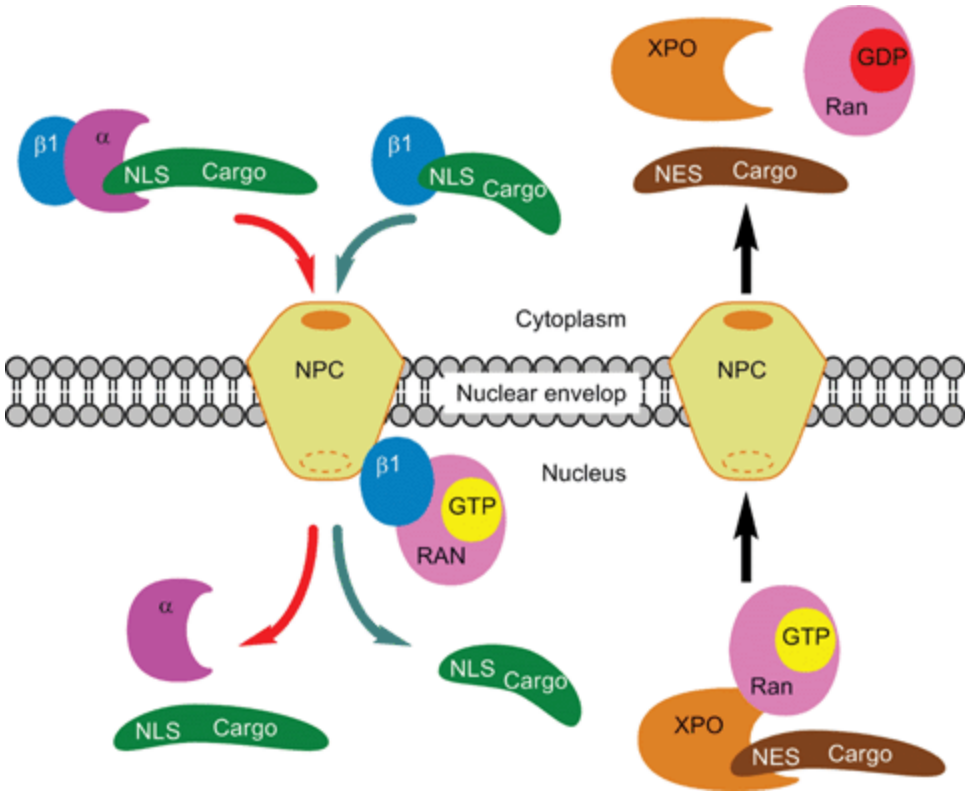

Figure 7. Nuclear import and export through the nuclear pore complex. Adapted from Okada et al. (2008)[71] with permission.

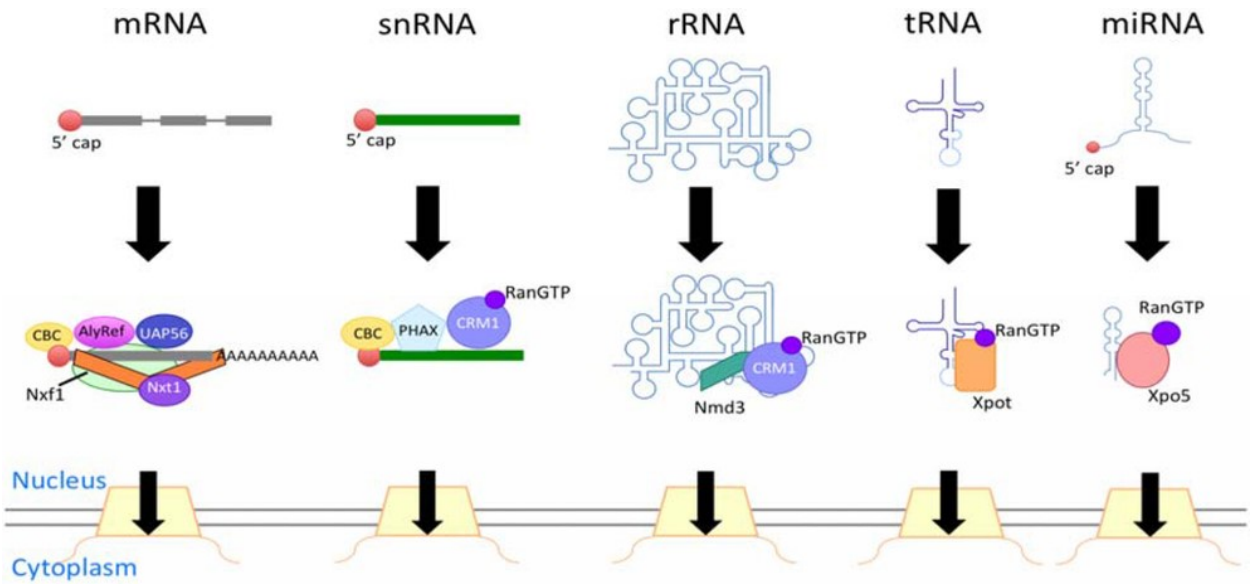

Figure 8. Main nuclear export pathways of RNAs. Adapted from Okamura et al. (2015)[72]

2. Aims and hypothesis

As discussed in section 1.2., co-doping increases the rate of excitation of the activator molecule and results in more intense emissions[36]. Here we co-doped unfunctionalized (Si-UCNP) or azide-functionalized (AzSi-UCNP) silica-coated $LiYF_4$ nanoparticles with two lanthanides: ytterbium (Yb^{3+}); an established sensitizer in upconversion spectroscopy[28,36,73]; thulium (Tm^{3+}), an established activator[27,73]. Excitation of Tm^{3+} with 980 nm wavelengths emits in the UV and visible part of the spectrum (Figure 9). Silica coating increases UCNP dispersibility in hydrophilic environments, prevents NP aggregation, and provides colloidal stability in biological environments. Silica is commonly used as a protective coat for particles with optical properties, such as quantum dots[74–76]. Azide-functionalization also increases stability of UCNPs in aqueous environments and allows for the conjugation of molecules to the surface of nanoparticles, by click chemistry between azides and alkynes.[28,77] This feature can be used to conjugate photocleavable molecules to the surface of UCNPs for controlled drug/gene delivery. Optimization of Tm^{3+} dopant concentration for maximal UV and visible emissions, characterization of UCNPs, and proof-of-concept experiments were previously published by our collaborators[27,28]. Briefly, proof-of-concept experiments were done in solution; results show controlled release of oligonucleotides clicked to azide-functionalized UCNPs, upon excitation with a 980 nm laser (Figure 10).

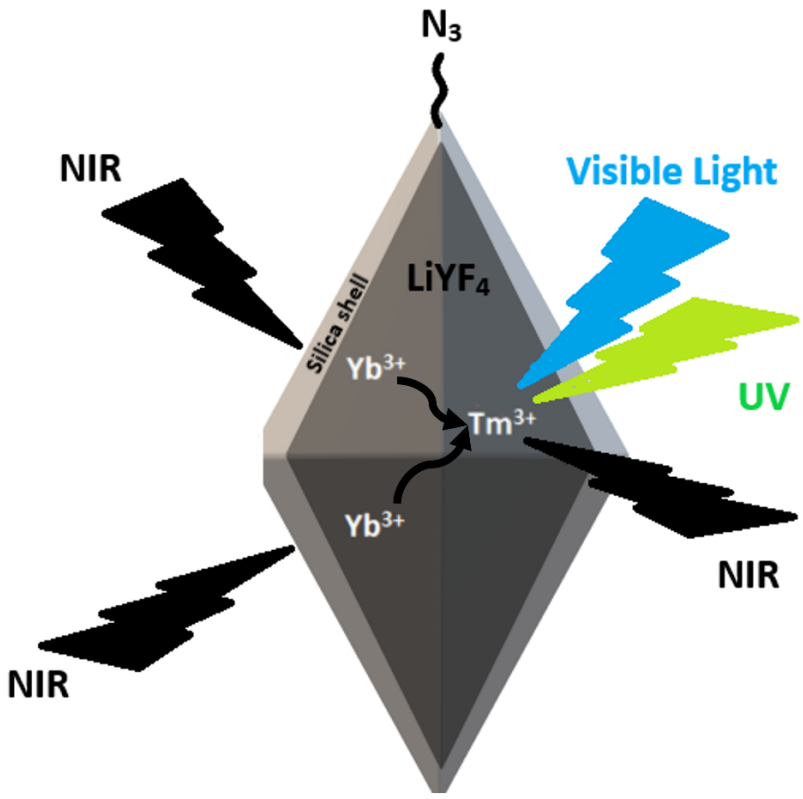

Figure 9. Graphical representation of unfunctionalized-silica coated UCNPs and azide-functionalized silica-coated UCNPs.

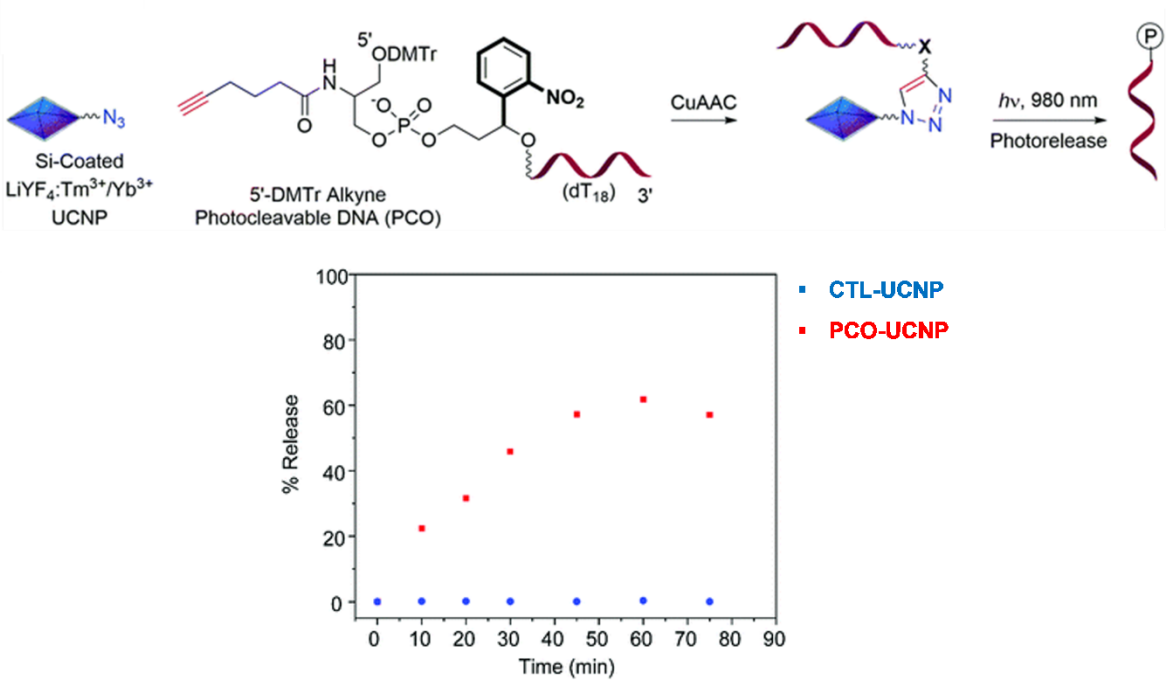

Figure 10. Proof-of concept of AzSi-UCNPs conjugated to oligonucleotides.The model shows the clicking of an alkyne base attached to a photocleavable oligonucleotide. Graph shows the controlled release of oligonucleotides upon excitation with 980 nm irradiation. Adapted from Liczner et al. (2021)[28] with permission.

As extensively discussed, use of UCNPs for diagnostics and therapeutics is hindered by their potential toxicity and varying physical properties. As such, newly developed nanoparticles must undergo extensive evaluation to determine their toxicity profile and subcellular interactions. *In vitro* studies, monitor the toxicity induced by nanoparticles through screening and evaluation of known hallmarks of stress. This is a prerequisite for future *in vivo* experiments to understand the potential toxic effects of our UCNPs.

Our UCNPs have unique physical properties and surface modifications and have not been studied in biological systems. Here, we use *in vitro* toxicity assays, immunofluorescence staining and Western blotting to assess the effects of Si-UCNPs and unconjugated AzSi-UCNPs on

healthy mammalian cells. We use two non-malignant mammalian cell lines: mouse embryonic fibroblasts (NIH3T3) and porcine kidney epithelial cells (LLC-PK1), as cell models. Fibroblasts are associated with several organs throughout the body; they function as homeostatic regulators and are involved in tissue damage repair.[78] Kidneys are involved in the excretion of waste from blood circulation and could potentially accumulate NPs.[30] Both NIH3T3 cells and LLC-PK1 cells are established cell lines in literature and their stress responses are well characterized. Hence, they are used as cell models in our toxicity assays. Introduction of UCNPs to a biological system can activate cell stress responses marked by changes in the physiological location or levels of nuclear and nucleolar proteins, transcription factors, molecular chaperones, nucleocytoplasmic shuttling proteins, pro-apoptotic markers or cytoskeletal organization[34,79].

2.1. Effects of UCNPs on cellular homeostasis

First, we set out to define the effects of our UCNPs, in the absence of irradiation, on cell viability and subcellular bio-nano interactions. We aim to achieve this by assessing the toxicity of Si-UCNPs and AzSi-UCNPs in NIH3T3 and LLC-PK1 cells and determining their effects on: 1) cytoskeletal organization; 2) oxidative stress responses; 3) the proteostasis network; and 4) nucleolar stress markers. We hypothesize that both Si-UCNPs and AzSi-UCNPs are non-toxic to both cell lines and will have minimal or no effects on the multiple stress markers studied. Results are shared in section 4.1.

2.2 Effects of UCNPs and their emissions on DNA damage and nuclear transport

Secondly, our objective is to determine the toxicity of the UCNPs after excitation with 980 nm irradiation. Also, we determine the effects of the UCNPs and their emissions on nucleic acid damage and nucleocytoplasmic transport. We aim to achieve this by 1) assessing the effects of emissions by excited Si-UCNPs and AzSi-UCNPs on NIH3T3 and LLC-PK1 cell viability; 2)

determining the effects of UCNPs and their emissions on DNA and RNA damage markers, and nucleocytoplasmic shuttling proteins. We hypothesize UCNPs and their emissions are non-toxic to both cell lines; they will have minimal or no effects on nucleic acids or nucleocytoplasmic transport. The results are shared in section 4.2. These are preliminary results and require further assessment by Western blotting and quantification of immunofluorescence signals.

3. Methods

3.1. UCNP synthesis and characterization

Nanoparticles composed of a $LiYF_4$ core shell, doped with 25 mol% Ytterbium and 0.2 mol% thulium were synthesized using a thermal decomposition technique. Nanoparticles were coated with unfunctionalized or azide-functionalized silica using the reverse microemulsion method. Characterization of nanoparticles properties by transmission electron microscopy (TEM), and evaluation of upconversion emission spectra and zeta potential was done by our collaborators following published protocols[28,80].

3.2. Cell culture

Mouse Embryonic Fibroblasts (NIH3T3) and Porcine Kidney Epithelial Cells (LLC-PK1) served as cell models in our experiments. Cells were cultured in Dulbecco's Modified Eagle Medium (DMEM) supplemented with 8% Bovine Calf Serum (BCS) and 1% Penicillin-Streptomycin (PEN/STREP) solution; they were incubated under standard growth conditions (37°C and 5% CO_2).

3.3. Cell seeding and treatment

3.3.1 Ln-UCNP treatment

Except for viability assays, cells were treated with 100 μg/mL Si-UCNPs or AzSi-UCNPs, for 24 hours. Sterile double-distilled water (ddH_2O) served as the vehicle control. First,

cells were seeded and incubated overnight. Following overnight incubation, cells were treated with sterile ddH_2O or Ln-UCNPs, at the indicated concentrations and exposure periods. Cells then reached 70% confluency and were processed for viability assays, immunofluorescence staining or Western blotting.

Aqueous Ln-UCNP stock solutions were vortexed until all precipitates were dissolved, then sonicated for 3 minutes at room temperature (Dare flow bath sonicator, PS-10A). The stock solution was diluted to 1 mg/mL in sterile ddH_2O, vortexed, and sonicated again for 2 minutes at room temperature. Then, diluted to the desired concentration in fresh DMEM. Finally, the seeded cells were treated with the diluted Ln-UCNPs, replacing the old medium, and incubated for the indicated exposure period.

3.3.2 Laser treatment

Where indicated, sterile ddH_2O or UCNP treated cells (as described in section 3.3.1) were irradiated using a 980 nm laser for 10 minutes at room temperature. Cells were then allowed to recover for 2 hours, under standard growth conditions. Unirradiated, sterile ddH_2O or Ln-UCNP treated cells, served as controls; they were placed at room temperature for 10 minutes, followed by a 2 hour recovery period. Cells were irradiated at a power density of 250 mW/cm^2, pulsed at 10 kHz using 10.5% duty cycle. Following the 2 hour recovery period, cells were processed for viability assays, immunofluorescence staining or Western blotting.

3.3.3. UV damage

To induce nucleic acid damage, cells were seeded on dishes or poly-lysine coated coverslips, incubated overnight, then treated with a UV-A lamp at 20 J/cm^2. Cells were then allowed to recover for the indicated time points and processed for Western blotting or

immunofluorescence staining. Controls were placed under similar conditions, in the absence of UV irradiation.

3.4. Viability assay

To test UCNP induced cytotoxicity, a resazurin based viability assay was used. Cells were grown in 96-well plates as described in section 3.3.1. Cells were treated with increasing concentrations of either Si-UCNPs or AzSi-UCNPs, ranging from 10 µg/mL to 100 µg/mL, for 24, 72 or 120 hours. Following treatment, cells were incubated with 25 µg/mL resazurin (Stock: 150 µg/mL resazurin in PBS) for 2-3 hours under standard growth conditions. Absorbance was then measured at 570 and 600 nm with a Tecan Infinite M1000 plate reader.

3.5. Immunofluorescence staining and imaging

For immunofluorescence staining, cells were grown on poly-L-lysine (0.01% in ddH_2O; air dried and sterilized under UV light for 3 hours) coated coverslips, as described in section 3.3.1. Following treatment with UCNPs for 24 hours, cells were washed with PBS, fixed with formaldehyde (3.7% in PBS) for 20 minutes at room temperature, and again washed with PBS. Next, cells were permeabilized (0.1% Triton X-100/PBS/2mg mL^{-1} BSA/1mM NaN_3) for 5 minutes and incubated with blocking buffer (0.05% Tween/PBS/5% BCS /1mM NaN_3) for 1 hour. Coverslips were then transferred to a humid chamber and incubated overnight with 50 µL of diluted primary antibodies (see tables 1 and 2 for antibody dilutions) at room temperature. Primary antibodies were diluted in blocking buffer and centrifuged (5 minutes; 13,000 rpm). Following overnight incubation, cells were washed with blocking buffer three times (5 minutes per wash), stained with 35 µL of diluted fluorescently labelled secondary antibodies for 2 hours and again washed three times with blocking buffer. Secondary antibodies were diluted in blocking buffer and centrifuged twice (5 minutes; 13,000 rpm), transferring the supernatant in

between spins. Finally, coverslips were stained with DAPI (1 μg/mL in blocking buffer) solution for 2 minutes, washed with PBS, mounted on microscope slides, and sealed with nail polish. Samples incubated with blocking buffer overnight (in the absence of primary antibodies) were stained with secondary antibodies to act as additional controls. Cy3- and alexaflour488-conjugated secondary antibodies were diluted 1:400, Cy3-conjugated secondary antibodies for Ran were diluted 1:500

For visualization of NIH 3T3 microtubules, using antibodies against α-tubulin, cells were fixed with ice-cold methanol for 15 minutes at -20°C then immediately incubated with blocking buffer for 1 hour at room temperature. Immunofluorescence staining follows the same procedure described above. For visualization of antibodies against γH2AX, the same procedure described above was followed. But cells were incubated with blocking buffer containing BSA instead of BCS (0.05% Tween/PBS/2 mg mL^{-1} BSA /1mM NaN_3).

Images were acquired using a Nikon optiphot or Nikon eclipse microscope equipped with a 40X objective. Identical settings were used to image individual data sets. A minimum of three independent experiments were performed for each antigen studied. A Zeiss LSM780-NLO laser scanning confocal, with IR-OPO lasers, microscope was used to image Ln-UCNPs by excitation at 976 nm.

3.5.1 Fluorescence quantification

Fluorescence signals were quantified using ImageJ. For each individual data set, a minimum of 30 cells were analyzed per treatment condition. Nuclear, cytoplasmic and/or whole cell mean intensity (intensity per area) were quantified for each cell and the average calculated. Values for cytoplasmic intensity and area were measured by calculating the difference between nuclear and whole cell intensity or area.

3.6. Western blotting

Cells were seeded on dishes and treated with UCNPs for 24 hours, UCNPs and laser irradiation or UV at the indicated time points (see section 3.3). Cell extraction and immunoblotting followed our previously published protocols[80,81]. Refer to table 1 for antibody dilutions.

3.7 Statistical Analysis

All quantified data was standardized to the vehicle control. Bar graphs for Western blotting and image analyses represent data averages for at least three independent experiments. Error bars are standard error of the means (SEM). A two-tailed Student's t-test or one-way ANOVA combined with Bonferroni correction were used to determine statistical significance between two or more groups, respectively. All figures show pairwise comparisons between the vehicle control and the treated sample. Significant differences are indicated as follows: *, $p < 0.05$; **, $p < 0.01$, and ***, $p < 0.001$.

Table 1. Immunofluorescence and Western blotting antibody dilutions related to results in section 4.1.

Antibody targets	Supplier, catalog number	Dilution for IF	Dilution for WB
Actin	Chemicon,MAB1501	NA	1:100,000
eIF2α	Santa Cruz Biotechn., sc-30882	NA	1:500
eIF2α	ABclonal, A0764	NA	1:500
phospho-eIF2α	Cell Signaling Techn., #3597	NA	1:500
Fibrillarin	Santa Cruz Biotechn., sc-25397	1:500	1:500
GAPDH	Santa Cruz Biotechn., SC-32233	NA	1:2,000
Grp78	Santa Cruz Biotechn., sc-13539	NA	1:1,000
Grp94	Santa Cruz Biotechn., sc-393402	NA	1:1,000
Hsp70	ENZO, ADI-SPA811	NA	1:2,000
Hsp90	Santa Cruz Biotechn., sc-515081	NA	1:500
Lamin A	Santa Cruz Biotechn., sc-20680	1:200	1:1,000
Lamin B	Santa Cruz Biotechn., sc-6216	1:400	1:1,000
NFκB	Santa Cruz Biotechn., sc-372	1:1000	1:500
Nrf2	Santa Cruz Biotechn., sc-365949	1:100	1:200
Nucleolin	Santa Cruz Biotechn., sc-13057	1:400	1:500
PARP1	ABclonal; A19596	NA	1:2,000
RPA194	Santa Cruz Biotechn., sc-48385	1:400	1:500
α-Tubulin	Santa Cruz Biotechn., sc-5286	1:200	1:1,000
VCP	BioLegend; No. 636802	NA	1:2,000
ZO-1	Santa Cruz Biotechn., sc-33725	1:200	NA

Table 2. Immunofluorescence antibody dilutions related to results in section 4.2.

Antibody targets	Supplier, catalog number	Dilution for IF
γH2AX	Millipore Sigma, 05-636	1:1000
Crm1	Santa Cruz Biotechn., sc-5595	1:400
RANGAP1	Santa Cruz Biotechn., sc-25630	1:2000
TAP/Nxf1	Santa Cruz Biotechn., sc-32319	1:800
KPNB1	Santa Cruz Biotechn., sc-11367	1:400
KPNA2	Santa Cruz Biotechn., sc-55538	1:400
RAN	Santa Cruz Biotechn., sc-1156	1:400
RPA194 (3T3/PK1)	Santa Cruz Biotechn., sc-48385	1:200/1:800
m6A	Santa Cruz Biotechn., sc-130219	1:1000
Nucleolin	Santa Cruz Biotechn., sc-13057	1:400

4. Results

4.1. Ln-UCNPs are non-toxic and have minimal effects on stress biomarkers in mammalian cells.

4.1.1 Ln-UCNP characterization

The UCNPs used are composed of a $LiYF_4$ core shell doped with the lanthanides Tm^{3+} and Yb^{3+}. As evidenced by TEM images (Figure 11 and Table 3), the nanoparticles have a square bipyramidal morphology with an average core length and width of 98.3 ± 6.5 and 52.3 ± 4.3, respectively. The emission spectra of UCNPs, measured in phenol-red free DMEM, showed the expected emissions in the UV and visible part of the spectrum (Figure 11c). Detailed properties of both Si-UCNPs and AzSi-UCNPs can be seen in table 3.

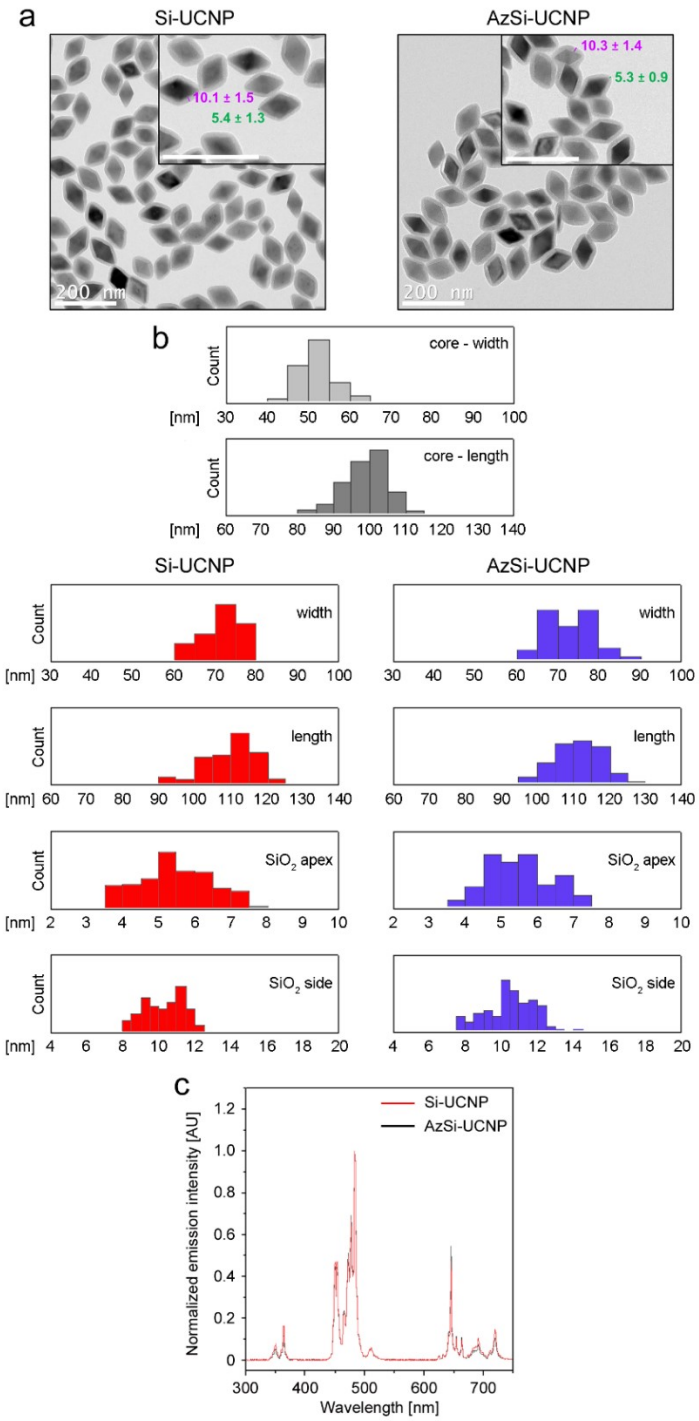

Figure 11. UCNP Characterization.a) Transmission electron microscopy images of Si-UCNP (left) and AzSi-UCNP (right). Silica shell thickness at the sides and apices is indicated in purple and green, respectively. Scale bar is 200 nm. b) Bar graphs depicting size distribution of core shell (grey) and Si-UCNPs or AzSi-UCNPs. c) Emission spectra of Si-UCNPs and AzSi-UCNPs

Table 3. Physical and chemical properties of UCNPs

Parameter	**Si-UCNP**	**AzSi-UCNP**
Host matrix	$LiYF_4$	
Sensitizer	25 mol% Yb^{3+}	
Activator	0.2 mol% Tm^{3+}	
Morphology	Square bipyramidal	
Core size; length [nm]	98.3 ± 6.5	
Core size; width [nm]	52.3 ± 4.3	
Size + shell, width [nm]	71.6 ± 4.8	73.0 ± 5.9
Shell thickness at edge [nm]	10.2 ± 1.1	10.4 ± 1.4
Shell thickness at apex [nm]	5.4 ± 1.0	5.5 ± 0.9
Zeta potential in water, 0.5 mg/mL UCNP [mV]	-11.5 ± 2.3	-16.3 ± 0.4
Zeta potential in DMEM, 0.5 mg/mL UCNP [mV]	-4.1 ± 0.1	-9.0 ± 0.5

4.1.2 Ln-UCNP cytotoxicity

Nanoparticle induced cytotoxicity was assessed after one, three or five days of exposure to varying concentrations of nanoparticles. After 24 hour incubation with UCNPs, the highest concentration of either Si- or AzSi-UCNPs did not elicit significant differences in cell viability, measured by cell metabolic activity (Figure 12). These results were similar for both NIH3T3 and LLC-PK1 cells. However, three and five days exposure to the nanoparticles showed a decrease in NIH 3T3 cell viability with increasing concentrations; these results were significant for 50 and

100 μg/mL concentrations. Three and five days UCNP treatment of LLC-PK1 cells did not show the same trend as NIH 3T3 cells (Figure 13). Since 24 hour treatment with the highest concentration of Si-UCNPs or AzSi-UCNPs showed no significant decrease in both NIH3T3 and LLC-PK1 cell viability, 100 μg/mL UCNPs for 24 hours was chosen in subsequent experiments to define the toxicity profile and subcellular interactions of our UCNPs.

PARP1 cleavage, marked by reduction in full-length PARP1 abundance, is an early marker of apoptosis[82]. To assess whether there are signs of UCNP induced apoptosis, PARP1 abundance levels were quantified by Western blotting. Immunoblot signals for PARP1 showed no decrease in either cell line, indicating no signs of UCNP induced apoptosis (Figure 12).

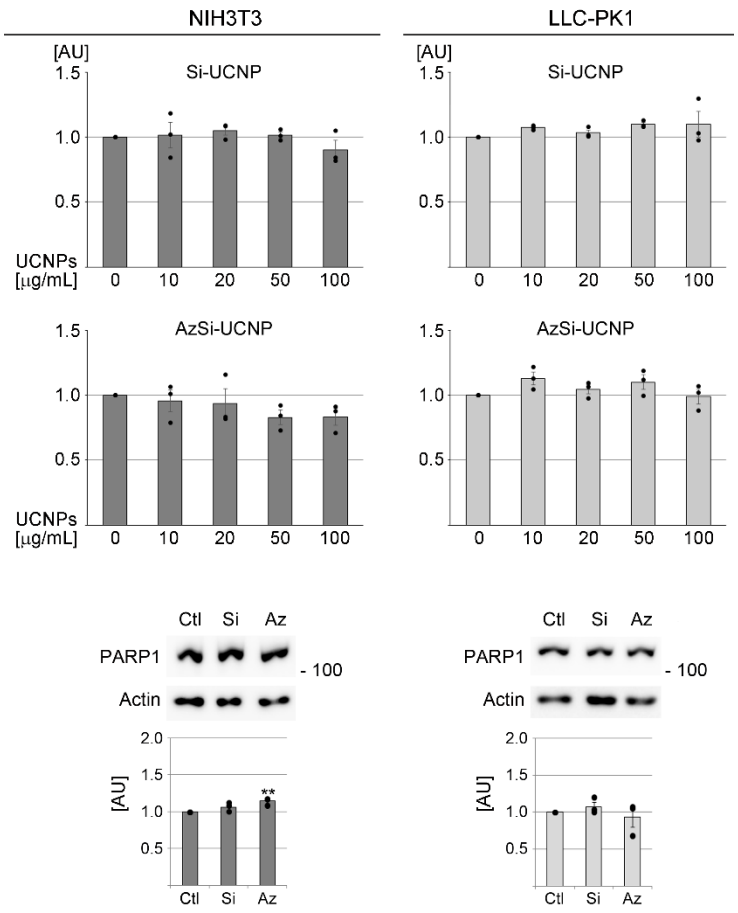

Figure 12. UCNP 24-hour cytotoxicity assays. Resazurin-based viability assays depicting changes in viability of NIH3T3 (left) and LLC-PK1 (right) cells upon 24-hours incubation with increasing concentrations of Si-UCNPs or AzSi-UCNPs. Western blots measured PARP1 abundance in both cell lines. The molecular mass (kD) of marker proteins is shown in the right margin of the blots. Bar graphs represent averages ± SEM of a minimum of three independent experiments. Results were normalized to vehicle control. Individual data points are shown as black circles. Statistical evaluation was performed with One-Way ANOVA and Bonferroni posthoc correction, $p < 0.01$. AU; arbitrary units.

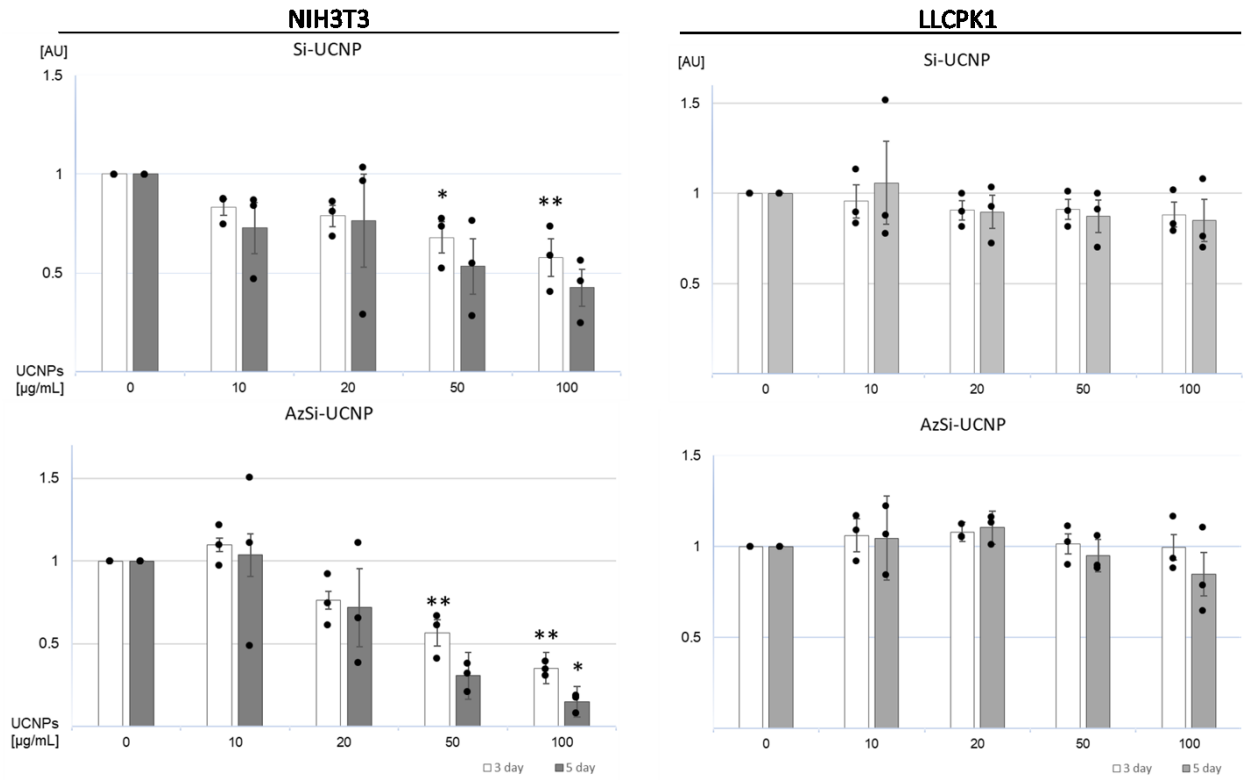

Figure 13. UCNP three day and five day cytotoxicity assays. Resazurin-based viability assays depicting changes in viability of NIH3T3 and LLC-PK1 cells upon 72- or 120-hours incubation with increasing concentrations of Si-UCNPs or AzSi-UCNPs. Bar graphs represent averages ± SEM of a minimum of three independent experiments. Results were normalized to vehicle control. Individual data points are shown as black circles. Statistical evaluation was performed with One-Way ANOVA and Bonferroni posthoc correction, *, $p < 0.05$; **, $p < 0.01$. AU; arbitrary units.

4.1.3 Ln-UCNP uptake

As seen in figure 11c, the UCNPs studied emit in the UV and visible light range when excited with 976 nm irradiation; this allows for their visualization within cells. To confirm interaction of the nanoparticles with cells after 24 hours of incubation, cells were treated with 100 µg/mL LnUCNPs for 24 hours, fixed and stained with the membrane marker, Zonula Occludens-1 (ZO-1). ZO-1 is a membrane protein associated with tight junctions in cells and serves as a good marker of cell periphery. Ln-UCNP uptake by NIH 3T3 and LLC-PK1 cells is evident by their association with cells (Figure 14). Both Si-UCNPs and AzSi-UCNPs were visualized within the cell periphery. Cells treated with the vehicle control showed no signals for UCNPs when visualized with the same channel settings (data not shown).

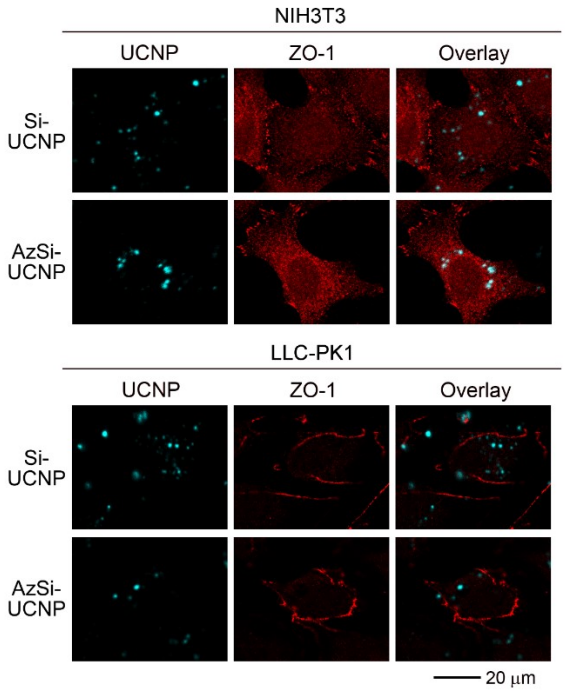

Figure 14. UCNP uptake. NIH3T3 fibroblasts and LLC-PK1 cells were incubated for 24 hours with 100 µg/mL Si-UCNP or AzSi-UCNPs. Cells were fixed and stained with antibodies against ZO-1. UCNPs were visualized after excitation 976 nm excitation. Scale bar is 20 µm.

4.1.4 Ln-UCNP effects on nuclear and cellular morphology

The cell structure and nuclear integrity are maintained by cytoskeletal proteins consisting of microtubules and nuclear lamins. Cell and nuclear morphology were unaffected by UCNP treatment after 24 hours (Figure 15, 16). However, Western blotting showed significant decreases in Lamin A and Lamin B in AzSi-UCNP treated NIH 3T3 cells. On the other hand, only Lamin B was significantly decreased in LLC-PK1 cells. These results might be early indicators of stress or cellular senescence due to subcellular interactions with azides on the UCNP surface.

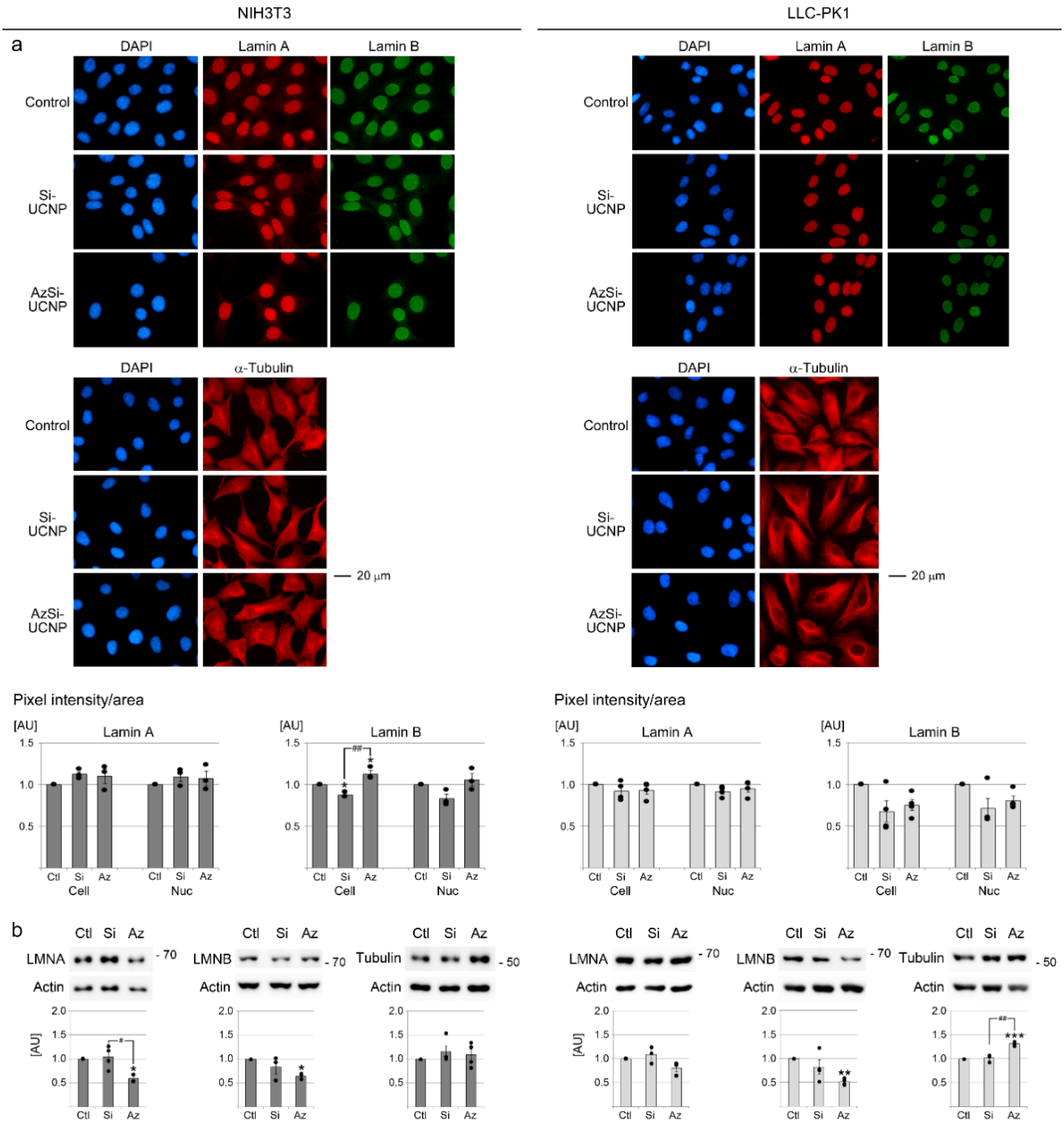

Figure 15. UCNP effects on nuclear and cell morphology. NIH3T3 and LLC-PK1 cells were incubated for 24 hours with vehicle, 100 μg/mL Si-UCNPs or AzSi-UCNPs. (a) The distribution of lamin A, lamin B or α-tubulin was monitored by immunolocalization. Whole cell and nuclear pixel intensities were quantified for three independent experiments. Scale bar is 20 μm. (b) The

abundance of lamin A, lamin B and α-tubulin was measured for at least three independent experiments. The molecular mass (kD) of marker proteins is shown in the right margin of the blots. (a, b) Bar graphs represent averages ± SEM of a minimum of three independent experiments. Results were normalized to vehicle controls. One-Way ANOVA combined with Bonferroni posthoc correction identified significant differences between the vehicle control group and individual treatment groups; *, $p < 0.05$, or between Si-UCNPs and AzSi-UCNPs; #, $p < 0.05$. AU, arbitrary units

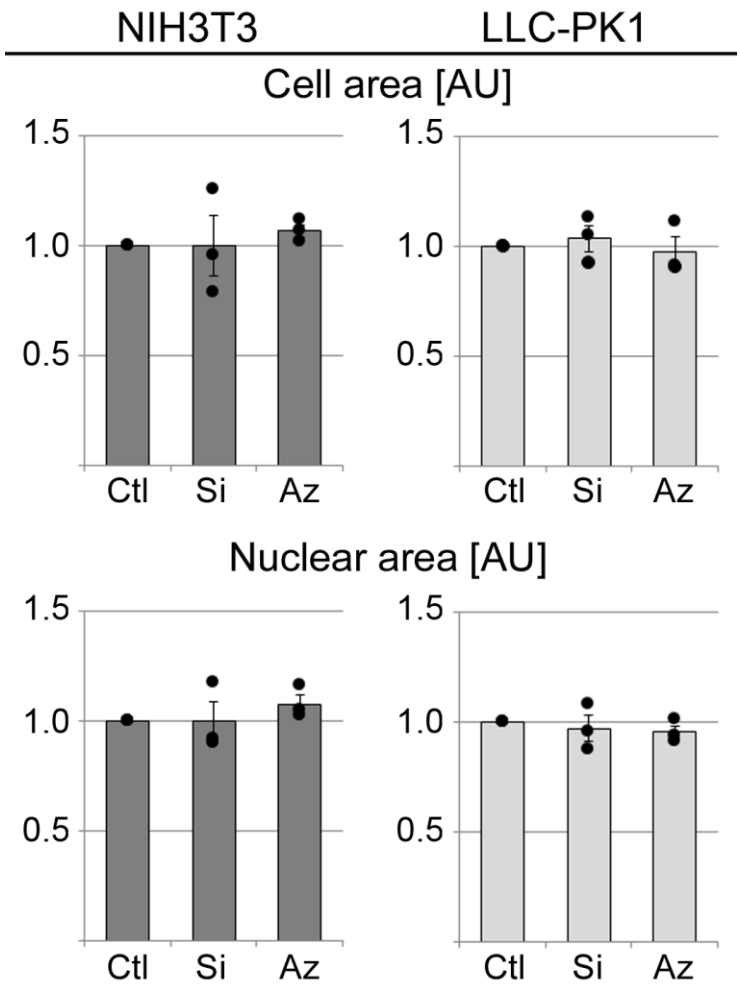

Figure 16. Effects of UCNPs on cell and nuclear area. NIH3T3 and LLC-PK1 cells were treated for 24 hours with vehicle, 100 µg/mL Si-UCNP or AzSi-UCNPs. Samples were fixed and processed for immunostaining. The size of cells and nuclei was quantified for three independent experiments. Results were normalized to vehicle controls. Bar graphs show averages ± SEM. No significant differences between control and treated samples were identified by One-Way ANOVA.

4.1.5 Ln-UCNP effects on oxidative stress and inflammatory markers

Cell response to oxidative stress is characterized by relocation of the transcription factors NF-κB and Nrf2 to the nucleus[53,83]. Immunofluorescence quantification of NF-κB and Nrf2 signals in the nucleus and cytoplasm showed no increase in the nucleocytoplasmic ratios of either protein in both cell lines. Moreover, Western blotting showed no severe changes in the abundance levels of both proteins, as well as the metabolic enzyme GAPDH[84]. Which has been shown to be a target of oxidative stress (Figure 17).

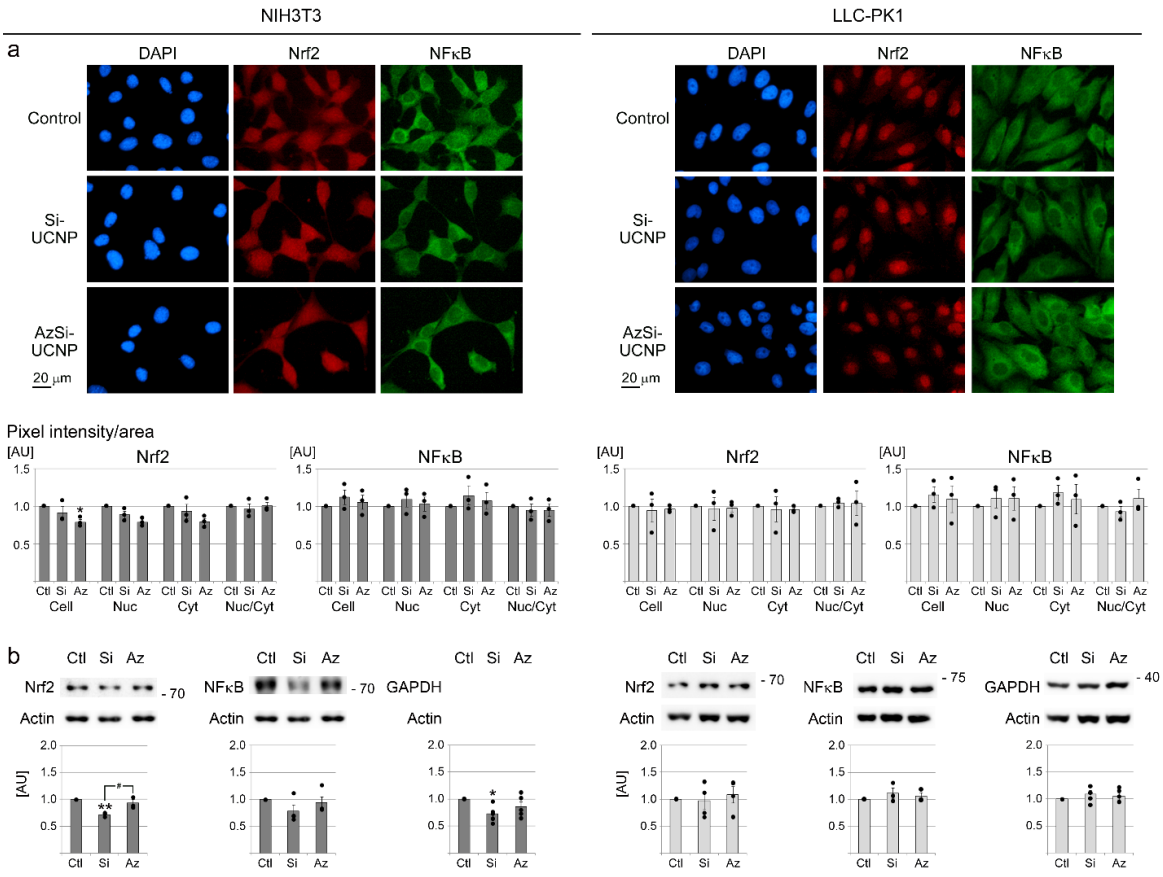

Figure 17. Effects of UCNPs on oxidative stress and inflammatory markers. NIH3T3 and LLC-PK1 cells were incubated for 24 hours with vehicle, 100 µg/mL Si-UCNPs or AzSi-UCNPs. (a) The distribution of Nrf2 and NF-κB was monitored by immunolocalization. Whole cell, nuclear and cytoplasmic pixel intensities were quantified for three independent experiments. Scale bar is 20 µm. (b) The abundance of Nrf2, NFκB, and GAPDH was measured for at least three independent experiments. The molecular mass (kD) of marker proteins is shown in the right margin of the blots. (a, b) Bar graphs represent averages ± SEM of a minimum of three independent experiments. Results were normalized to vehicle controls. One-Way ANOVA combined with Bonferroni posthoc correction identified significant differences between the vehicle control group and individual treatment groups; *, $p < 0.05$; **$p < 0.01$, or between Si-UCNPs and AzSi-UCNPs; #, $p < 0.05$. AU, arbitrary units

4.1.6 Ln-UCNP effects on nucleolar stress response

Nucleoli are sensitive stress indicators due to their dynamic structure and critical role in RNA biosynthesis. As mentioned, the events of rRNA transcription, processing and assembly are distinctively compartmentalized in nucleoli. RPA194, the major catalytic subunit of RNA Pol I[85], Fibrillarin, an RNP involved in pre-rRNA methylation and processing[86]; and nucleolin "C23", an RNA and DNA binding protein located mainly in the granular compartment and involved in RNA assembly were used to mark the distinctive nucleolar compartments[87]. As evidenced by IF staining (Figure 18), nucleolar integrity was unaffected by UCNP treatment in either cell. However, nucleolin was significantly decreased in both Si-UCNP and AzSi-UCNP treated NIH3T3 cells suggesting possible impairment in rRNA processing or DNA replication. This might affect the proliferative capacity of cells.

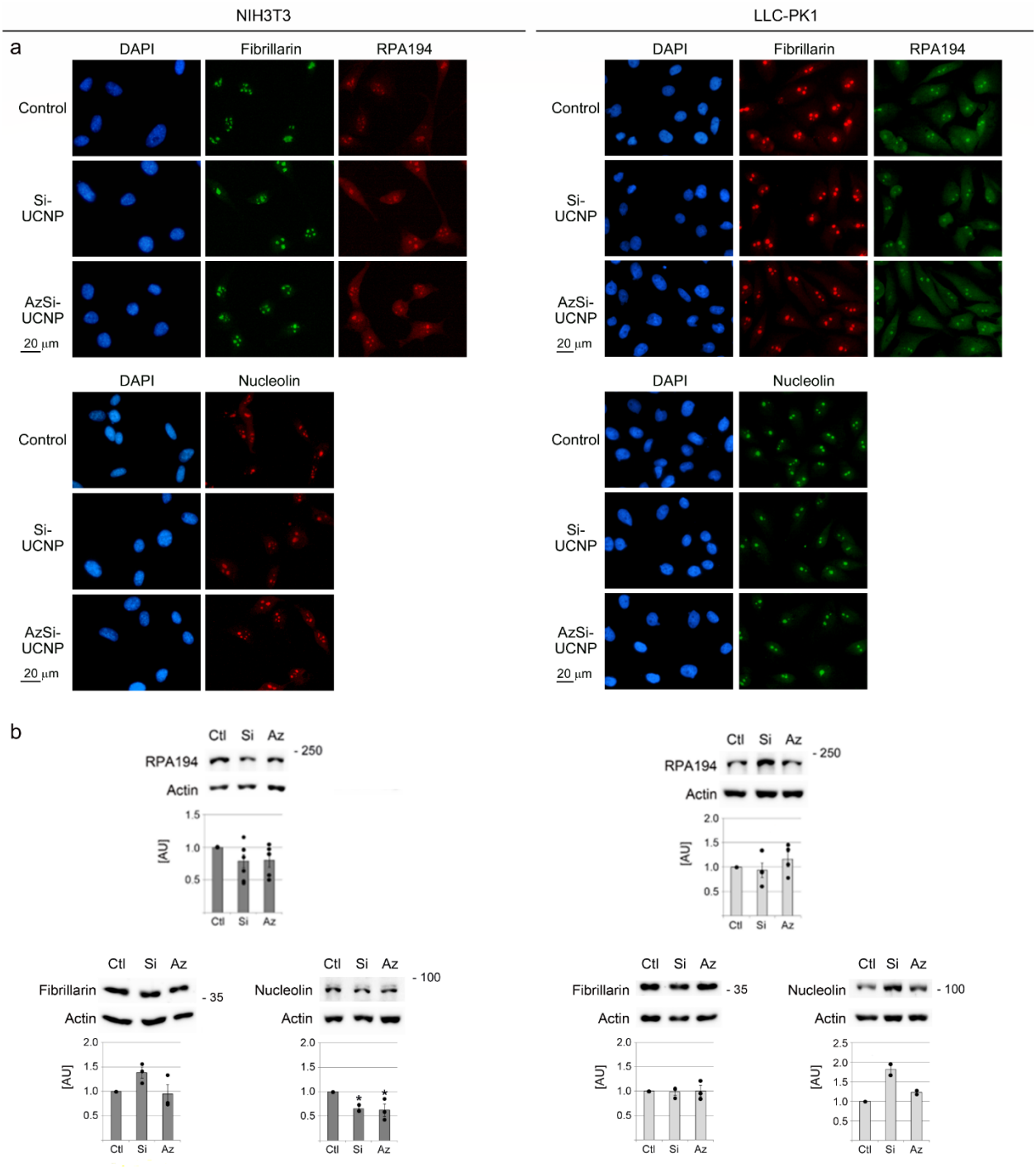

Figure 18. Effects of UCNPs on nucleolar stress markers. NIH3T3 and LLC-PK1 cells were incubated for 24 hours with vehicle, 100 µg/mL Si-UCNPs or AzSi-UCNPs. (a) The distribution of RPA194, fibrillarin, and nucleolin was monitored by immunolocalization. Scale bar is 20 µm. (b) The abundance of RPA194, fibrillarin, and nucleolin was measured. The molecular mass (kD)

of marker proteins is shown in the right margin of the blots. Bar graphs represent averages ± SEM of a minimum of three independent experiments. Results were normalized to vehicle controls. One-Way ANOVA combined with Bonferroni posthoc correction identified significant differences between the vehicle control group and individual treatment groups; *, $p < 0.05$. AU, arbitrary units

4.1.7. Ln-UCNP effects on ER stress response and molecular chaperones

The untranslated protein response is a mechanism developed by cells to withstand stress. Under severe ER stress, cells have been shown to induce apoptosis and inhibit cell cycle progression[39]. A hallmark of the UPR response is elevated ER stress response proteins and molecular chaperones involved in protein folding. Here we tested the levels of several proteins involved in the UPR to determine early markers of induction of apoptosis or cell cycle arrest[88]. Western blotting showed no significant changes for ER related stress response proteins (Figure 19). However, the molecular chaperone, Hsp70 was significantly increased in response to AzSi-UCNP in both cell lines, although, the increase was more significant in NIH3T3 cells (2-fold increase in NIH3T3 cells compared to a 1.2 fold increase in LLC-PK1 cells). A significant increase in Hsp90 levels was observed in both Si-UCNP and AzSi-UCNP treated LLC-PK1 cells but not NIH3T3 cells.

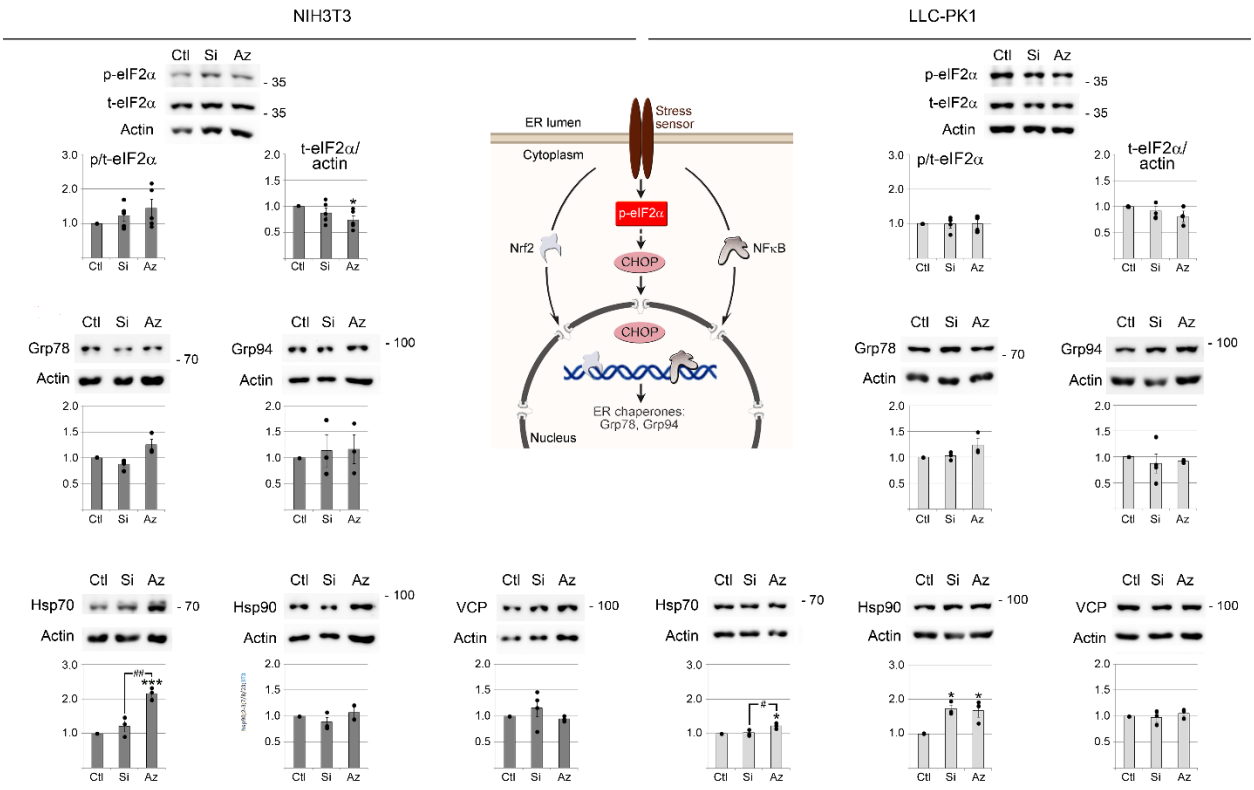

Figure 19. Effects of UCNPs on ER stress markers and the proteostasis network. NIH3T3 and LLC-PK1 cells were incubated for 24 hours with vehicle, 100 µg/mL Si-UCNPs or AzSi-UCNPs. The abundance of phosphorylated and total-eIF2α, Grp78, Grp94, Hsp70, Hsp90 and VCP was measured. The molecular mass (kD) of marker proteins is shown in the right margin of the blots. Bar graphs represent averages ± SEM of a minimum of three independent experiments. Results were normalized to vehicle controls. One-Way ANOVA combined with Bonferroni posthoc correction identified significant differences between the vehicle control group and individual treatment groups; *, $p < 0.05$; **$p < 0.01$ *; ***$p < 0.001$. AU, arbitrary units

4.2. Ln-UCNPs affect nucleocytoplasmic shuttling proteins in mammalian cells; their excitation has minimal effects on nucleic acid damage and other stress responses.

4.2.1. Ln-UCNP emissions are non-cytotoxic

Ln-UCNPs and their emissions could result in genotoxic stress by production of reactive oxygen species, hypermethylation of RNA or by formation of DNA breaks. Recruitment of DNA damage repair proteins varies in different cell lines. To establish time points for DNA and RNA damage markers in our cell lines we performed genotoxicity assays with multiple recovery time points. Given that the UCNPs emit in the UV-A range (~360 nm), we irradiated cells with 20 J/cm2 of 360 nm UV light, in the absence of UCNPs. Results showed the highest increase in γH2AX fluorescence 2 hours after recovery (Figure 20).

To test the potential cytotoxicity of the UCNP emissions we performed viability assays on a range of concentrations after 24 hours of incubation with UCNPs, followed by their excitation for 10 minutes and a 2 hour recovery period. No decrease in cell viability was observed for the highest concentration of UCNPs tested (Figure 21). Genotoxicity was marked by the DNA repair protein γH2AX and methylated RNA. No changes in γH2AX fluorescence intensity was observed after treatment with UCNPs, with and without laser irradiation (Figure 22). m6A staining shows no obvious changes in location or intensity upon treatment with UCNPs or laser irradiation (Figure 23). However, these results need to be confirmed by IF quantification.

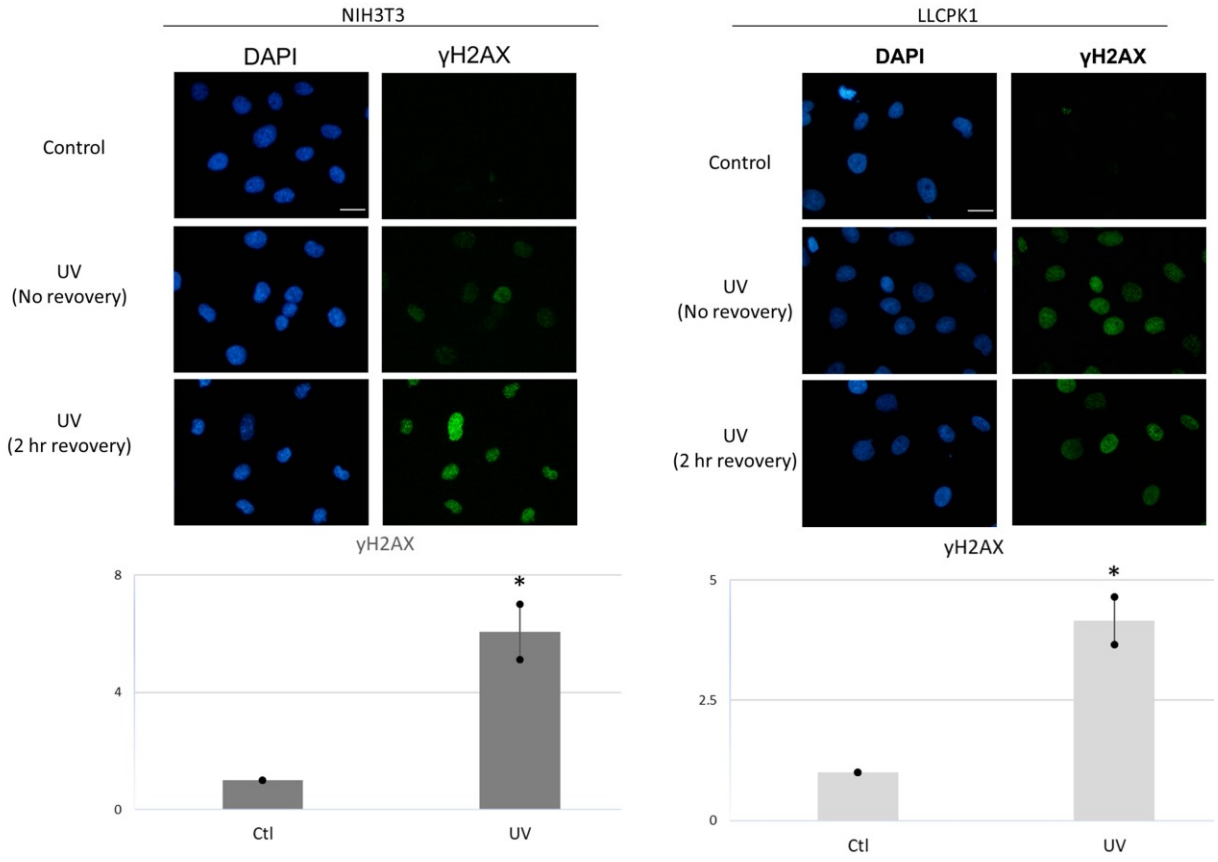

Figure 20. UV effects on DNA damage markers. NIH3T3 and LLC-PK1 cells were treated with 20 J/cm^2 of UV-A light and allowed to recover for 0 or 2 hours (a) The distribution of γH2AX was monitored by immunolocalization. Nuclear pixel intensity was quantified for control and UV treated+2 hour recovery for two independent experiments. Scale bar is 20 µm. Bar graphs represent averages ± SEM of a minimum of three independent experiments. Results were normalized to vehicle controls. Black circles represent individual data points. Student's t-test identified significant differences between the vehicle control group and the treated group; *, $p <$ 0.05. AU, arbitrary units

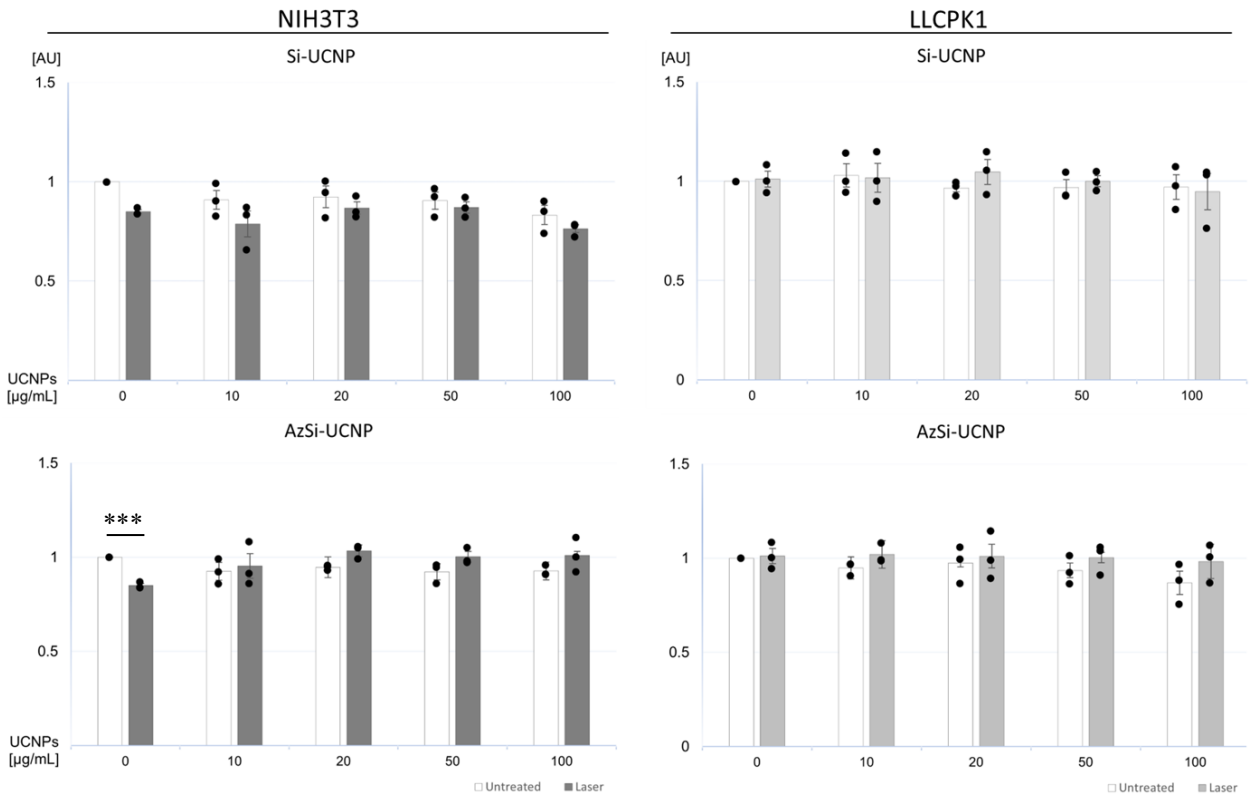

Figure 21. Cytotoxic effects of UCNP emissions. Resazurin-based viability assays depicting changes in viability of NIH3T3 (left) and LLC-PK1 (right) cells upon 24-hours incubation with increasing concentrations of Si-UCNPs or AzSi-UCNPs, with (white bars) and without irradiation. Bar graphs represent averages ± SEM of a minimum of three independent experiments. Results were normalized to vehicle control. Individual data points are shown as black circles. No significant differences were identified with One-Way ANOVA. Student's t-test identified significant differences between irradiated and unirradiated groups at similar concentrations. $P < 0.001$. AU; arbitrary units.

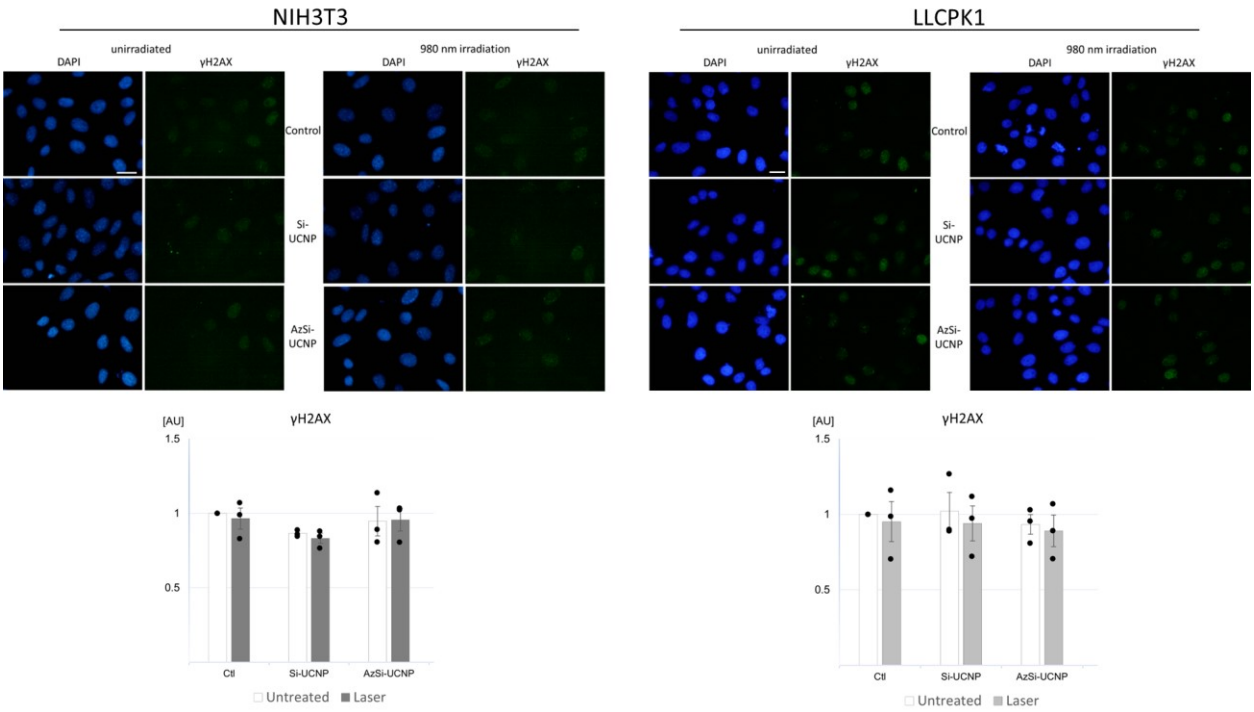

Figure 22. Effects of UCNPs and their emissions on DNA damage markers. NIH3T3 and LLC-PK1 cells were incubated for 24 hours with vehicle, 100 µg/mL Si-UCNPs or AzSi-UCNPs, +/- 980 nm excitation, and allowed to recover for 2 hours (a) The distribution of γH2AX was monitored by immunolocalization. Nuclear pixel intensity was quantified three independent experiments. Scale bar is 20 µm. Bar graphs represent averages ± SEM of a minimum of three independent experiments. Results were normalized to vehicle controls. Black circles represent individual data points. One-Way ANOVA combined with Bonferroni identified significant differences between the vehicle control group and the treated group; *, $p < 0.05$. AU; arbitrary units

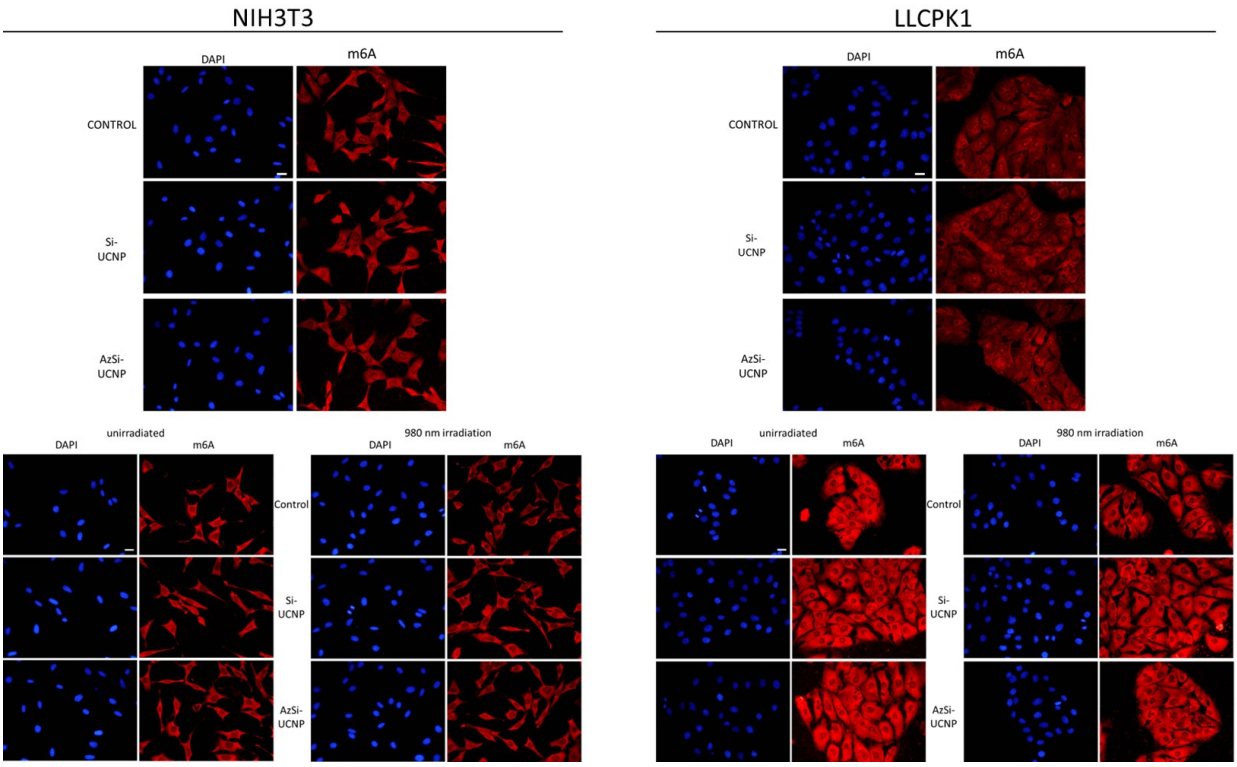

Figure 23. Effects of UCNPs and their emissions on RNA methylation. NIH3T3 and LLC-PK1 cells were incubated for 24 hours with vehicle, 100 µg/mL Si-UCNPs or AzSi-UCNPs, or incubated for 24 hours with vehicle, 100 µg/mL Si-UCNPs or AzSi-UCNPs, +/- 980 nm excitation, and allowed to recover for 2 hours. The distribution of m6A was monitored by immunolocalization. Scale bar is 20 µm.

4.2.2 Ln-UCNP effects on nuclear import and export

The transport of molecules between the nucleus and the cytoplasm is a requirement for maintenance of cellular homeostasis. Nuclear import and export was assessed in both cell lines. Crm1 relocated to nucleoli (marked by RPA194) upon Si-UCNP or AzSi-UCNP treatment of NIH 3T3 cells. In LLC-PK1 controls, CRM1 is distributed in the nucleoplasm and associated with nucleolar bodies, there was no observed increase in CRM1 nucleolar bodies upon UCNP treatment. On the other hand, TAP/Nxf1 aggregated in the cytoplasm of UCNP treated LLC-PK1

cells but not NIH3T3 fibroblasts (Figure 24). No changes in the location of importins was observed for either cell line (Figure 25). Both Importin αβ dependent nuclear import and CRM1 dependent nuclear export are Ran-dependent. As such, we stained treated cells with Ran. In accordance with the literature both cell lines showed higher concentrations of Ran in the nucleus. Treatment with UCNPs did not cause changes in the subcellular location of Ran. RanGAP1 is one of two enzymes responsible for maintaining the Ran gradient across the nucleocytoplasm[89,90]. Treatment with UCNPs also had no effects on the subcellular location of RanGAP1 (Figure 24). These results suggest that the observed effects in NIH3T3 cells might not be Ran-dependent.

Next, we assessed whether excitation of UCNPs would exacerbate the results observed with unirradiated UCNPs. Relative to unirradiated UCNP treatment, excitation of UCNPs did not have observable effects on the nuclear import and export proteins. Suggesting that the UCNP emissions do not exacerbate effects of UCNPs on nucleocytoplasmic shuttling (Figure 26 and 27).

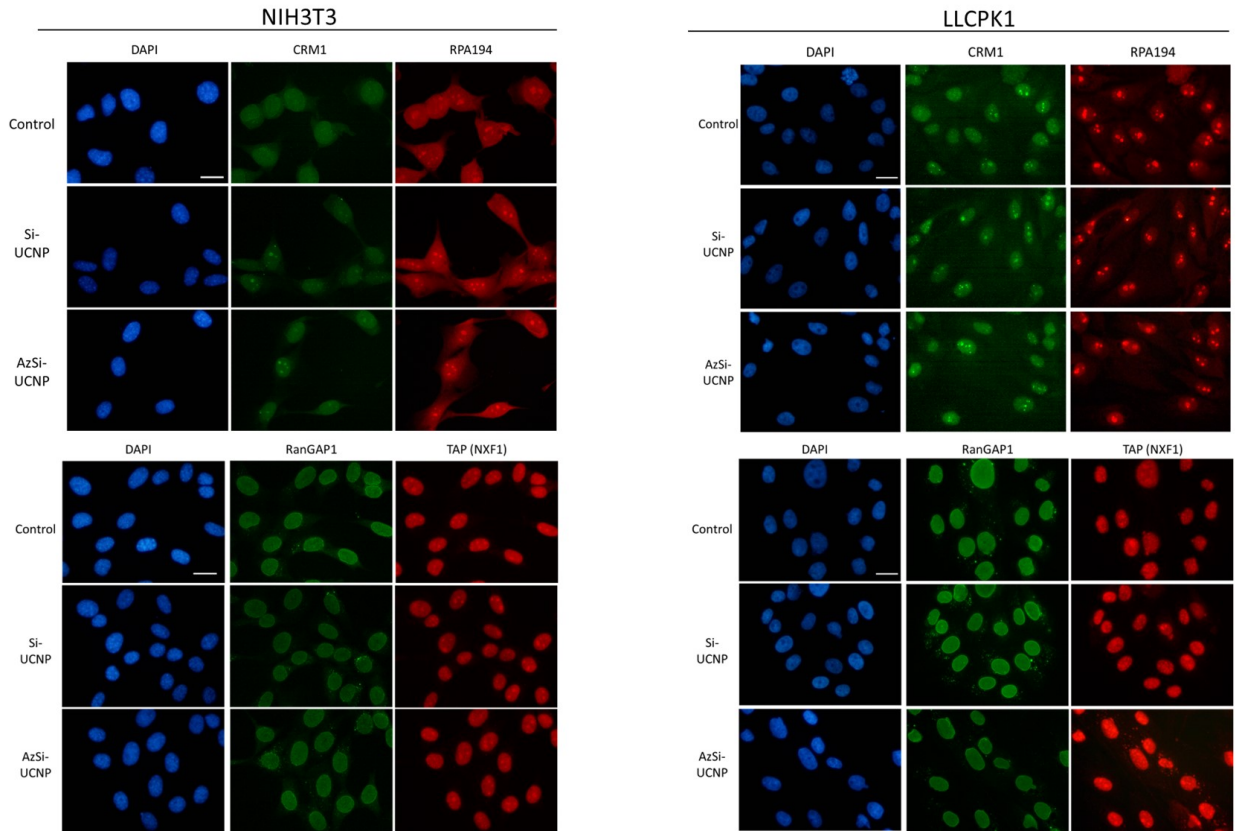

Figure 24. Effects of UCNPs on nuclear export proteins. NIH3T3 and LLC-PK1 cells were incubated for 24 hours with vehicle, 100 µg/mL Si-UCNPs or AzSi-UCNPs. The distribution of CRM1, RPA194, RANGAP1 AND TAP/Nxf1 was monitored by immunolocalization. Scale bar is 20 µm.

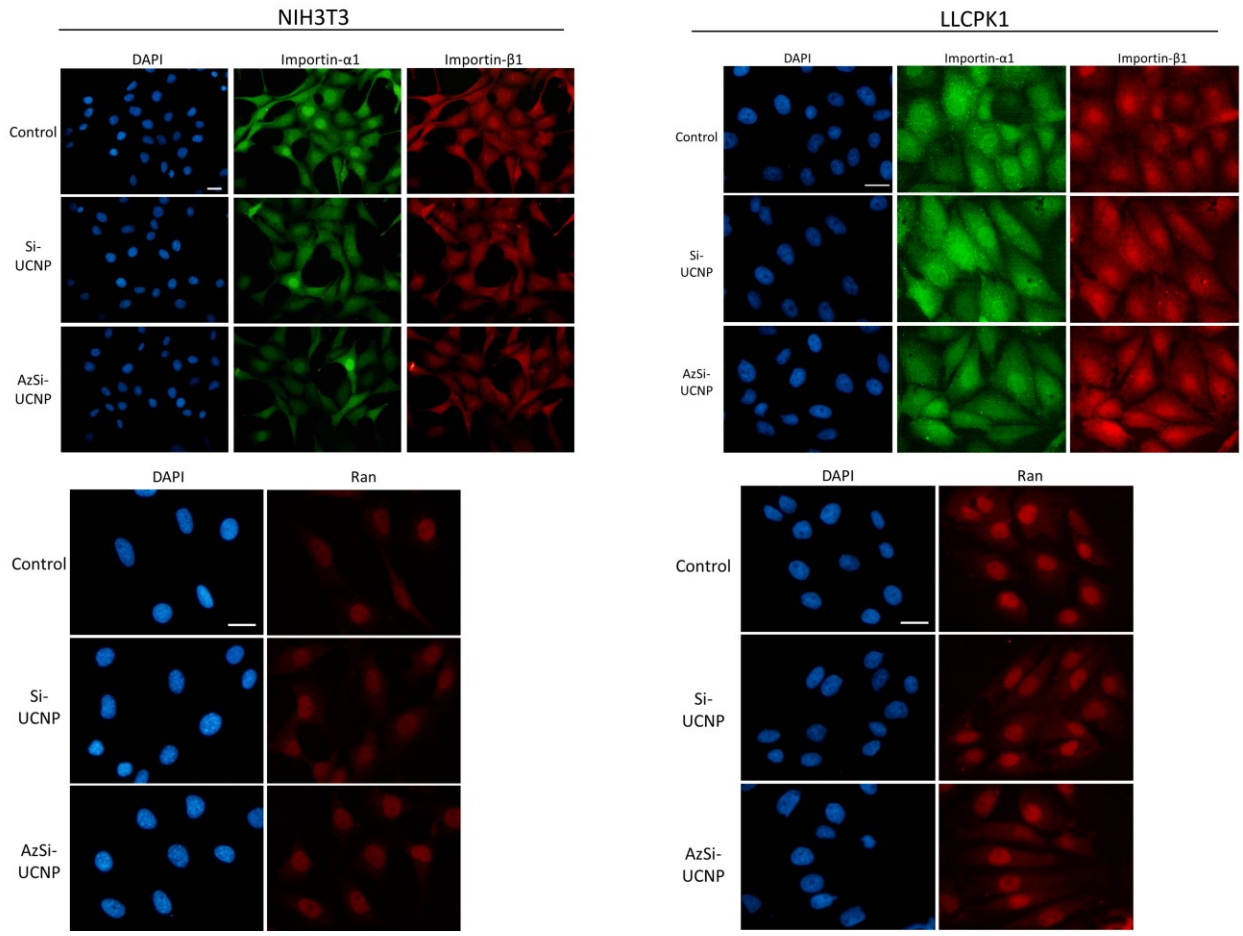

Figure 25. Effects of UCNPs on importins and Ran. NIH3T3 and LLC-PK1 cells were incubated for 24 hours with vehicle, 100 µg/mL Si-UCNPs or AzSi-UCNPs. The distribution of importin-α_1, importin-β_1 and Ran was monitored by immunolocalization. Scale bar is 20 µm.

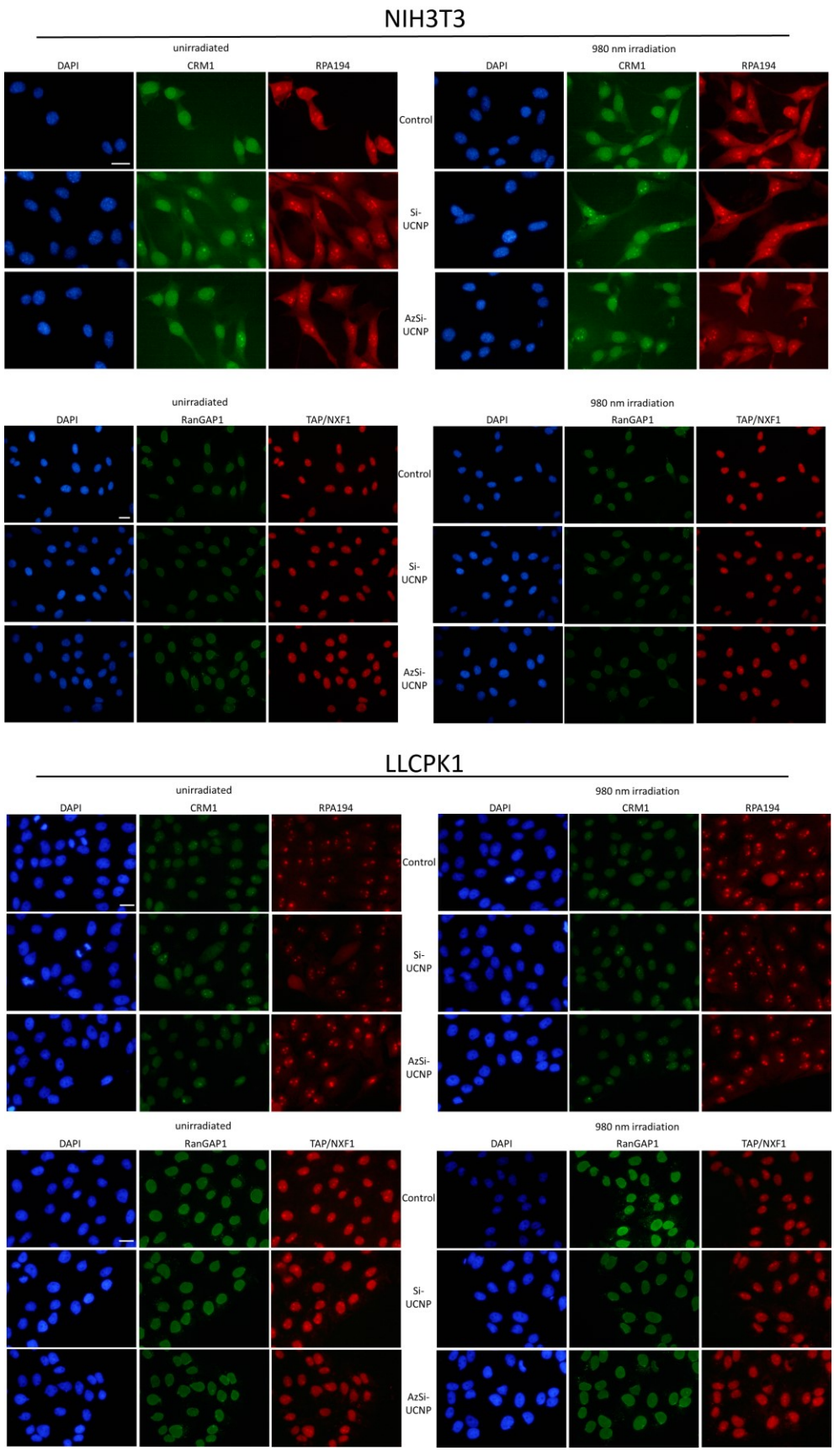
NIH3T3
unirradiated
980 nm irradiation
DAPI
CRM1
RPA194
Control
Si-UCNP
AzSi-UCNP
RanGAP1
TAP/NXF1
LLCPK1

Figure 26. Effects of UCNP emissions on nuclear export proteins. NIH3T3 and LLC-PK1 cells were incubated for 24 hours with vehicle, 100 µg/mL Si-UCNPs or AzSi-UCNPs, +/- 980 nm irradiation and allowed to recover for 2 hours. The distribution of CRM1, RPA194, RANGAP1 AND TAP/Nxf1 was monitored by immunolocalization. Scale bar is 20 µm.

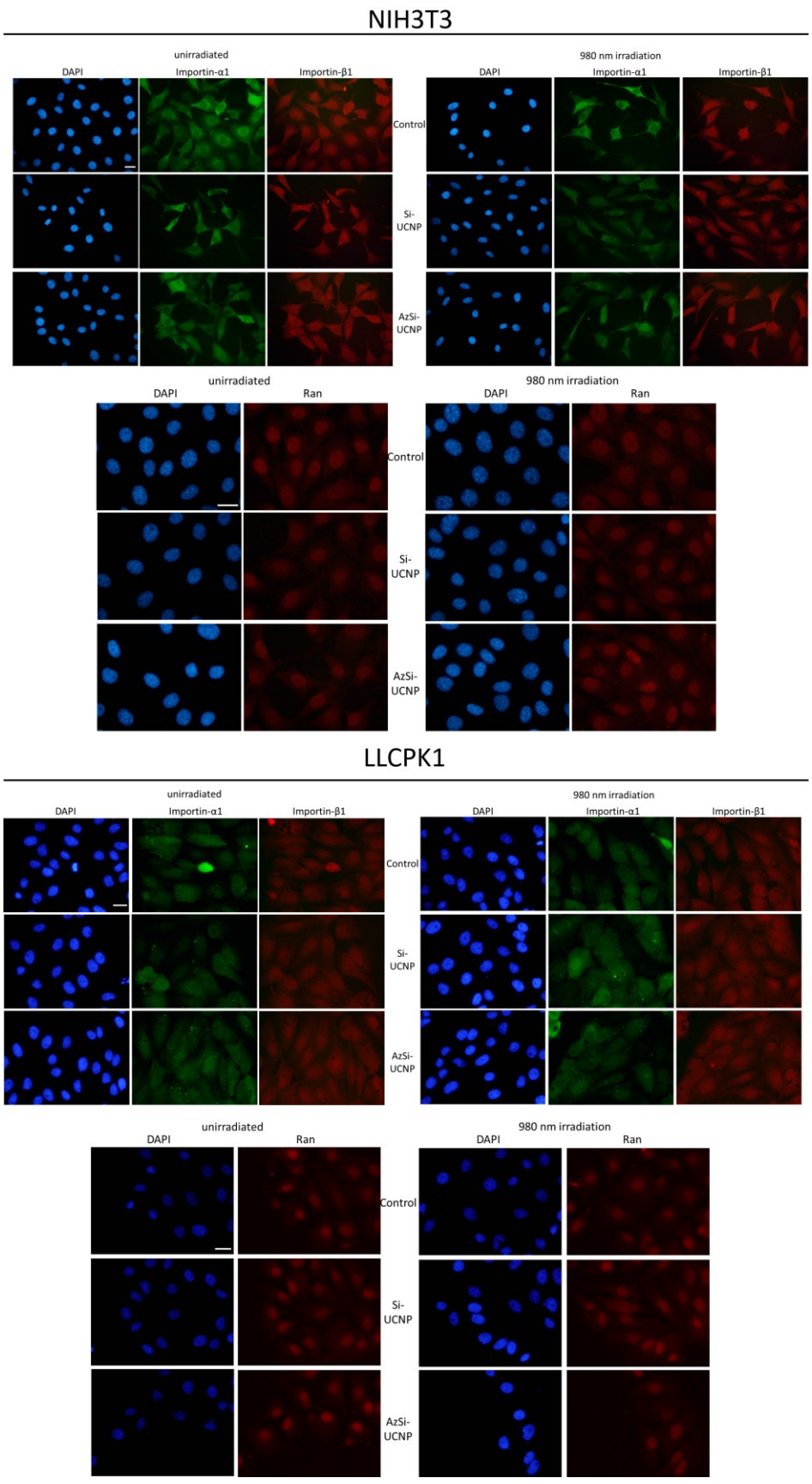
NIH3T3
unirradiated
980 nm irradiation
DAPI
Importin-α1
Importin-β1
Control
Si-UCNP
AzSi-UCNP
DAPI
Ran
LLCPK1

Figure 27. Effects of UCNP emissions on importins and Ran. NIH3T3 and LLC-PK1 cells were incubated for 24 hours with vehicle, 100 μg/mL Si-UCNPs or AzSi-UCNPs, +/- 980 nm irradiation and allowed to recover for 2 hours. The distribution of importin-α_1, importin-β_1 and Ran was monitored by immunolocalization. Scale bar is 20 μm.

5. Discussion

5.1. Ln-UCNPs have minimal cytotoxic effects after 24 hours

We investigated the effects of upconversion nanoparticles (UCNPs) on NIH3T3 and LLC-PK1 cells to understand the cellular responses. The results at 24 hours indicated a lack of immediate cytotoxicity, as evidenced by the absence of a decrease in cell viability in both cell lines. Surprisingly, the longer-term assessments at 72 and 120 hours revealed a significant decrease in cell viability specifically in NIH3T3 cells. These differences in cell responses emphasize the dynamic nature of cellular reactions to UCNPs over extended exposure periods, highlighting the importance of considering the duration of nanoparticle exposure in toxicity assessments. The reaction was more severe in AzSi-UCNP treated cell. However, the lack of apoptotic markers at 24 hours could be indicative of an inhibition of cell proliferation.

The elevation of Hsp70 in both cell lines at 24 hours implies an early cellular stress response, to mitigate the impact of UCNPs. One paper, reports an increase in Hsp70 levels in repsonse to treatment with sodium azides[91]. Azide is a metabolic inhibitor and could result in the observed decrease with NIH3T3 treated AzSi-UCNPs over prolonged periods.

5.2. Ln-UCNPs have minimal, cell type specific, effects on cellular stress responses

Proteins elevated during ER stress are essential for induction of autophagy to withstand stress. Pre-treatment with tunicamycin, a known ER stressor, had a protective effect on LLCPK1 cells after hypoxia treatment. Knockdown of proteins mediating ER stress in mouse embryonic fibroblasts resulted in cell death[39]. However, under severe ER stress, cells have been shown to induce apoptosis and cell cycle arrest by decreasing proteins involved in cell cycle progression. Particularly, in NIH3T3 cells, known ER stressors like tunicamycin decreased Cyclin D1 protein

synthesis and the protein was undetectable by western blotting 16 hours after exposure to the drug[88].

Conclusions in relation to proteins involved in nucleoctoplasmic shuttling are limited due to incomplete results. Without proper quantification of protein abundance by Western blotting and quantification of the RAN gradient it is difficult to draw definitive conclusions. Preliminary results show changes in the localization of two important export proteins, Crm1 and Nxf1; however, their relocation was cell type specific. Nucleoporins and transport proteins, such as importins and exportins, work closely to ensure the stability of the nuclear pore complex. [70]Importins and exportins are major driving components in the maintenance of cellular homeostasis. Abnormalities in the shuttling of proteins and nucleic acids to and from the nucleus can have a negative impact on cells. Major export proteins CRM1 and Nxf1 are critical for the transport of ribosomal RNA and mRNA from the nucleus to the cytoplasm. Importin α and β are responsible for the movement of molecules containing a NLS from the cytoplasm to the nucleus Communication between the nucleus and cytoplasm occurs through these proteins. Disruption of the nuclear or cytoplasmic concentrations of importins and exportins can lead to anti-apoptotic activities.[69]

NIH 3T3 cells shows a trend of decrease for RPA194, and other nucleolar factors were also affected when treated with Si-UCNPs or AzSi-UCNPs. The main cargo in CRM1 export pathways is processed rRNA. The relocation of Crm1 to nucleoli in NIH3T3 cells could be attributed to a decrease in processed rRNA, because of RNA polymerase I inhibition or malfunctioned processing of newly synthesized rRNA. It has been previously shown that specific inhibition of RNA polymerase I with drugs, such as short exposure to low concentrations of actinomycin D, relocates CRM1 to nucleoli[92–94]. A previously published study by our lab

reported changes in importin αβ levels but not CRM1 in LLC-PK1 cells treated with POEGA-b-PMAEP coated $NaYF_4$ UCNPs[80].

On the other hand, LLCPK1 cells showed sequestration of Nxf1 in the cytoplasm of Si-UCNP and AzSi-UCNP treated cells. The main cargo in TAP/Nxf1 export pathways is mRNA. Inhibition of ribosomal translation could result in the accumulation of mRNA and, potentially, its exporter, in the cytoplasm of cells. One paper reported on the proteomics analysis of effects of silver nanoparticles on lung, breast and colon epithelial cells. The results of the analysis also showed cell type specific effects. Where Nxf1 protein expression levels were significantly altered in only lung epithelial cells[95,96].

Another paper assessed the effects of gold nanoparticles functionalized with an NLS signal and reported accumulation of the NLS-AuNP on the cytoplasmic side of the nuclear periphery of HeLa cells, blocking nuclear import and export, which resulted in non-apoptotic cell death by induction of autophagosomes and autolysosomes. Similarly, treatment with agglutinin, a nuclear complex inhibitor, also resulted in a similar phenotype[97]. Hence, the results from our study might indicate that NIH3T3 decrease in cell viability after three and five days was via a non-apoptotic pathway due to inhibition of nuclear export evidenced by CRM1 relocation to nucleoli and accumulation of UCNPs around the nuclear periphery of NIH3T3 cells.

Transcription and translation assays determining the synthetization, and proper processing and folding of nascent rRNA and mRNA are required to define the possible mechanisms for the observed cell type specific phenotypes.

5.3. Ln-UCNPs and their emissions do not affect DNA and RNA damage markers, and do not exacerbate observed Ln-UCNP effects on nucleocytoplasmic shuttling.

DNA and RNA damage could occur in response to UCNP induced genotoxicity by production of ROS or by their UV emissions. H2AX phosphorylation is an ideal marker of DNA damage. However, this process is dynamic and varies for different cell lines, and modes of stress. Since our UCNPs emit in the UV part of the spectrum we used UV-A to induce γ-H2AX. Phosphorylation of H2AX upon UV-A treatment established a 2-hour recovery period is optimal for both NIH3T3 and LLCPK1 cells. To our knowledge, there are no reports on the dynamics of γ-H2AX in NIH 3T3 or LLC-PK1 cells upon irradiation with UV-A light. Other papers reported on effects of metal-based NPs on γ-H2AX in malignant cell lines, showing increased formation of double strand breaks by ROS activation[98]. Here, we do not see an effect of the UCNPs or their emissions on formation of double strand breaks. RNA methylation is an important post-transcriptional modification, of which N^6-methyladenosine (m^6A) is the most abundant. This process is closely linked to RNA splicing, however alterations in methylation have been shown to affect RNA export and translation[99,100]. Hence, we assessed the effects of UCNP treatment on this process; m^6A has been shown to be affected by nanoparticle treatments[101]. Wang et al. (2022), reported on the increase in m^6A in kidney and lung cells after exposure to quantum dots, this was accompanied by severe ER stress[102].

5.4. Future directions

The results displayed assess specific stress biomarkers after 24 hour incubation with the nanoparticles; Our knowledge of the bio-nano interactions after a prolonged incubation period is limited. Further studies at different time points and with the introduction of recovery periods are necessary to increase our understanding of the effects induced by the nanoparticles. Moreover,

identifying the mechanism of internalization of the UCNPs is beneficial to understand the physiological relevance of the time points studied.

The experiments conducted in this research studied the effects of irradiated and unirradiated Si-UCNPs and AzSi-UCNPs in the absence of a photocleavable biomolecule. Proof of concept studies were performed with oligonucleotides clicked to the Azide functionalized UCNPs in solution. The effects of these biomolecules when introduced into cells should be further studied as the release profile could be different in cells compared to solution. Moreover, the results in this experiment highlighted the cell type specific differences induced by the UCNPs. Therefore, their toxic effects and subcellular interactions need to be studied with other relevant mammalian cell types such as immune cells, hepatic cells and splenocytes as they can accumulate nanoparticles involved in the collection of nanoparticles from blood circulation[10,18,30]. Nanoparticles of this size and shape are understudied in living organisms; their circulation times, properties and toxic effects need to be investigated in the context of *in vivo* experiments.

Conclusion

Previous work by our collaborators optimized the properties of the UCNPs used in this study and demonstrated the functional application of AzSi-UCNPs as drug delivery tools. However, the use of these nanoparticles in living cells and their cytotoxicity was unknown. We performed a variety of *in vitro* toxicity assays evaluating various pathways that are relevant to nanoparticle induced stress. Here we showed minimal UCNP effects on nuclear envelope proteins, molecular chaperones and nucleolar stress markers. We demonstrated the UCNP induced relocation of major nucleocytoplasmic transport factors. Finally, we proved the minimal cytotoxic and genotoxic effects of emissions by excited UCNPs. Our research is the first to define the toxicity and subcellular interactions of LiYF4: Yb^{3+}, Tm^{3+} UCNPs. The results obtained highlight the cell type specific effects of nanoparticles. These results provide a framework for future *in vivo* experiments. Further work is required to understand the mechanisms and implications of the observed changes.

References

1. Nanotechnology and engineered nanomaterials are at the forefront of development and innovation [1-4]. Nanomaterials are omnipresent; they are indispensable for basic research (biose- nsors, nanorobotics), health (bioimaging, diagnostics, therapeutics),. :1-2.
2. Peng D, Fu M, Wang M, Wei Y, Wei X. Targeting TGF-β signal transduction for fibrosis and cancer therapy. *Molecular Cancer 2022 21:1*. 2022;21(1):1-20. doi:10.1186/S12943-022-01569-X
3. Kim BG, Malek E, Choi SH, Ignatz-Hoover JJ, Driscoll JJ. Novel therapies emerging in oncology to target the TGF-β pathway. *Journal of Hematology & Oncology 2021 14:1*. 2021;14(1):1-20. doi:10.1186/S13045-021-01053-X
4. Maia A, Wiemann S. Cancer-Associated Fibroblasts: Implications for Cancer Therapy. *Cancers (Basel)*. 2021;13(14). doi:10.3390/CANCERS13143526
5. Sengar P, Juárez P, Verdugo-Meza A, et al. Development of a functionalized UV-emitting nanocomposite for the treatment of cancer using indirect photodynamic therapy. *J Nanobiotechnology*. 2018;16(1):1-19. doi:10.1186/S12951-018-0344-3/FIGURES/9
6. Gessner I, Neundorf I. Nanoparticles Modified with Cell-Penetrating Peptides: Conjugation Mechanisms, Physicochemical Properties, and Application in Cancer Diagnosis and Therapy. *International Journal of Molecular Sciences 2020, Vol 21, Page 2536*. 2020;21(7):2536. doi:10.3390/IJMS21072536
7. Anselmo AC, Mitragotri S. Nanoparticles in the clinic: An update. *Bioeng Transl Med*. 2019;4(3). doi:10.1002/BTM2.10143
8. Anselmo AC, Mitragotri S. Nanoparticles in the clinic. *Bioeng Transl Med*. 2016;1(1):10. doi:10.1002/BTM2.10003

9. Namiot ED, Sokolov A V., Chubarev VN, Tarasov V V., Schiöth HB. Nanoparticles in Clinical Trials: Analysis of Clinical Trials, FDA Approvals and Use for COVID-19 Vaccines. *International Journal of Molecular Sciences 2023, Vol 24, Page 787*. 2023;24(1):787. doi:10.3390/IJMS24010787

10. Zhu GH, Gray ABC, Patra HK. Nanomedicine: controlling nanoparticle clearance for translational success. *Trends Pharmacol Sci*. 2022;43(9):709-711. doi:10.1016/J.TIPS.2022.05.001

11. Dong H, Du SR, Zheng XY, et al. Lanthanide Nanoparticles: From Design toward Bioimaging and Therapy. *Chem Rev*. 2015;115(19):10725-10815. doi:10.1021/ACS.CHEMREV.5B00091/ASSET/IMAGES/LARGE/CR-2015-00091Y_0048.JPEG

12. Mitchell MJ, Billingsley MM, Haley RM, Wechsler ME, Peppas NA, Langer R. Engineering precision nanoparticles for drug delivery. *Nature Reviews Drug Discovery 2020 20:2*. 2020;20(2):101-124. doi:10.1038/s41573-020-0090-8

13. Rizwan M, Shoukat A, Ayub A, Razzaq B, Tahir MB. Types and classification of nanomaterials. *Nanomaterials: Synthesis, Characterization, Hazards and Safety*. Published online January 1, 2021:31-54. doi:10.1016/B978-0-12-823823-3.00001-X

14. Altammar KA. A review on nanoparticles: characteristics, synthesis, applications, and challenges. *Front Microbiol*. 2023;14:1155622. doi:10.3389/FMICB.2023.1155622/BIBTEX

15. Harish V, Tewari D, Gaur M, et al. Review on Nanoparticles and Nanostructured Materials: Bioimaging, Biosensing, Drug Delivery, Tissue Engineering, Antimicrobial, and Agro-Food Applications. *Nanomaterials*. 2022;12(3). doi:10.3390/NANO12030457

16. Gessner I, Neundorf I. Nanoparticles Modified with Cell-Penetrating Peptides: Conjugation Mechanisms, Physicochemical Properties, and Application in Cancer Diagnosis and Therapy. *International Journal of Molecular Sciences 2020, Vol 21, Page 2536*. 2020;21(7):2536. doi:10.3390/IJMS21072536

17. Rashid EU, Nawaz S, Munawar J, et al. Organic and inorganic nanoparticles. *Smart Polymer Nanocomposites: Design, Synthesis, Functionalization, Properties, and Applications*. Published online January 1, 2023:93-119. doi:10.1016/B978-0-323-91611-0.00014-1

18. Sharma N, Bietar K, Stochaj U. Targeting nanoparticles to malignant tumors. *Biochimica et Biophysica Acta (BBA) - Reviews on Cancer*. 2022;1877(3):188703. doi:10.1016/J.BBCAN.2022.188703

19. Sedlmeier A, Gorris HH. Surface modification and characterization of photon-upconverting nanoparticles for bioanalytical applications. *Chem Soc Rev*. 2015;44(6):1526-1560. doi:10.1039/c4cs00186a

20. Cheng X, Zhou J, Yue J, et al. Recent Development in Sensitizers for Lanthanide-Doped Upconversion Luminescence. *Chem Rev*. 2022;122(21):15998-16050. doi:10.1021/ACS.CHEMREV.1C00772/ASSET/IMAGES/LARGE/CR1C00772_0045.JPEG

21. Lee G, Park Y Il. Lanthanide-Doped Upconversion Nanocarriers for Drug and Gene Delivery. *Nanomaterials*. 2018;8(7). doi:10.3390/NANO8070511

22. Dutta R, Barik P. Upconversion and Downconversion Quantum Dots for Biomedical and Therapeutic Applications. *Application of Quantum Dots in Biology and Medicine: Recent*

Advances. Published online January 1, 2022:229-263. doi:10.1007/978-981-19-3144-4_12/FIGURES/7

23. Malhotra K, Hrovat D, Kumar B, et al. Lanthanide-Doped Upconversion Nanoparticles: Exploring A Treasure Trove of NIR-Mediated Emerging Applications. *ACS Appl Mater Interfaces*. Published online 2022. doi:10.1021/ACSAMI.2C12370/ASSET/IMAGES/LARGE/AM2C12370_0011.JPEG
24. Mi P. Stimuli-responsive nanocarriers for drug delivery, tumor imaging, therapy and theranostics. *Theranostics*. 2020;10(10):4557. doi:10.7150/THNO.38069
25. Gupta A, Weng Lam C, Ting Wu C, et al. Photothermal Disintegration of 3T3 Derived Fat Droplets by Irradiated Silica Coated Upconversion Nanoparticles. *Particle & Particle Systems Characterization*. 2018;35(12):1800294. doi:10.1002/PPSC.201800294
26. Dukhno O, Przybilla F, Collot M, et al. Quantitative assessment of energy transfer in upconverting nanoparticles grafted with organic dyes. *Nanoscale*. 2017;9(33):11994-12004. doi:10.1039/c6nr09706e
27. Maurizio SL, Tessitore G, Mandl GA, Capobianco JA. Luminescence dynamics and enhancement of the UV and visible emissions of Tm3+ in LiYF4:Yb3+,Tm3+ upconverting nanoparticles. *Nanoscale Adv*. 2019;1(11):4492-4500. doi:10.1039/C9NA00556K
28. Liczner C, Mandl GA, Maurizio SL, Duke K, Capobianco JA, Wilds CJ. Synthesis and fundamental studies of a photoresponsive oligonucleotide-upconverting nanoparticle covalent conjugate. *Mater Chem Front*. 2021;5(12):4690-4699. doi:10.1039/D1QM00467K

29. Jalani G, Naccache R, Rosenzweig DH, et al. Real-time, non-invasive monitoring of hydrogel degradation using LiYF 4 :Yb 3+ /Tm 3+ NIR-to-NIR upconverting nanoparticles. *Nanoscale*. 2015;7(26):11255-11262. doi:10.1039/C5NR02482J

30. Zhang A, Meng K, Liu Y, et al. Absorption, distribution, metabolism, and excretion of nanocarriers in vivo and their influences. *Adv Colloid Interface Sci*. 2020;284:102261. doi:10.1016/J.CIS.2020.102261

31. Hoshyar N, Gray S, Han H, Bao G. The effect of nanoparticle size on in vivo pharmacokinetics and cellular interaction. *Nanomedicine*. 2016;11(6):673. doi:10.2217/NNM.16.5

32. Kettler K, Veltman K, van de Meent D, van Wezel A, Hendriks AJ. Cellular uptake of nanoparticles as determined by particle properties, experimental conditions, and cell type. *Environ Toxicol Chem*. 2014;33(3):481-492. doi:10.1002/ETC.2470

33. Rojas-Gutierrez PA, Bekah D, Seuntjens J, Dewolf C, Capobianco JA. Cellular Uptake, Cytotoxicity and Trafficking of Supported Lipid-Bilayer-Coated Lanthanide Upconverting Nanoparticles in Alveolar Lung Cancer Cells. *ACS Appl Bio Mater*. 2019;2(10):4527-4536. doi:10.1021/ACSABM.9B00649/ASSET/IMAGES/LARGE/MT9B00649_0007.JPEG

34. Khan AA, Allemailem KS, Almatroudi A, et al. Endoplasmic Reticulum Stress Provocation by Different Nanoparticles: An Innovative Approach to Manage the Cancer and Other Common Diseases. *Molecules 2020, Vol 25, Page 5336*. 2020;25(22):5336. doi:10.3390/MOLECULES25225336

35. Fleischer CC, Payne CK. Nanoparticle-cell interactions: Molecular structure of the protein corona and cellular outcomes. *Acc Chem Res*. 2014;47(8):2651-2659. doi:10.1021/AR500190Q

36. Liu C, Sun S, Mao J. Water-soluble Yb3+, Er3+ codoped NaYF4 nanoparticles induced SGC-7901 cell apoptosis through mitochondrial dysfunction and ROS-mediated ER stress. *Hum Exp Toxicol*. 2023;42:1-10. doi:10.1177/09603271231188493

37. Kodiha M, Mahboubi H, Maysinger D, Stochaj U. Gold Nanoparticles Impinge on Nucleoli and the Stress Response in MCF7 Breast Cancer Cells. *Nanobiomedicine (Rij)*. 2016;3. doi:10.5772/62337

38. Manke A, Wang L, Rojanasakul Y. Mechanisms of nanoparticle-induced oxidative stress and toxicity. *Biomed Res Int*. 2013;2013. doi:10.1155/2013/942916

39. Chandrika BB, Yang C, Ou Y, et al. Endoplasmic Reticulum Stress-Induced Autophagy Provides Cytoprotection from Chemical Hypoxia and Oxidant Injury and Ameliorates Renal Ischemia-Reperfusion Injury. *PLoS One*. 2015;10(10):140025. doi:10.1371/JOURNAL.PONE.0140025

40. Thiruvengadam R, Venkidasamy B, Samynathan R, Govindasamy R, Thiruvengadam M, Kim JH. Association of nanoparticles and Nrf2 with various oxidative stress-mediated diseases. *Chem Biol Interact*. 2023;380:110535. doi:10.1016/J.CBI.2023.110535

41. Min Y, Suminda GGD, Heo Y, Kim M, Ghosh M, Son YO. Metal-Based Nanoparticles and Their Relevant Consequences on Cytotoxicity Cascade and Induced Oxidative Stress. *Antioxidants 2023, Vol 12, Page 703*. 2023;12(3):703. doi:10.3390/ANTIOX12030703

42. Savage DT, Hilt JZ, Dziubla TD. In Vitro Methods for Assessing Nanoparticle Toxicity. *Methods Mol Biol*. 2019;1894:1. doi:10.1007/978-1-4939-8916-4_1

43. Kumar V, Sharma N, Maitra SS. In vitro and in vivo toxicity assessment of nanoparticles. *International Nano Letters 2017 7:4*. 2017;7(4):243-256. doi:10.1007/S40089-017-0221-3

44. 14: The Cytoskeleton - Biology LibreTexts. Accessed February 14, 2021. https://bio.libretexts.org/Courses/University_of_California_Davis/BIS_2A%3A_Introductory_Biology_(Easlon)/Readings/14%3A_The_Cytoskeleton

45. Moujaber O, Stochaj U. The Cytoskeleton as Regulator of Cell Signaling Pathways. *Trends Biochem Sci*. 2020;45(2):96-107. doi:10.1016/j.tibs.2019.11.003

46. Lambert MW. The functional importance of lamins, actin, myosin, spectrin and the LINC complex in DNA repair. *Exp Biol Med*. 2019;244(15):1382-1406. doi:10.1177/1535370219876651

47. Freund A, Laberge RM, Demaria M, Campisi J. Lamin B1 loss is a senescence-associated biomarker. *Mol Biol Cell*. 2012;23(11):2066. doi:10.1091/MBC.E11-10-0884

48. Chu S, Moujaber O, Lemay S, Stochaj U. Multiple pathways promote microtubule stabilization in senescent intestinal epithelial cells. *npj Aging 2022 8:1*. 2022;8(1):1-12. doi:10.1038/s41514-022-00097-8

49. Ispanixtlahuatl-Meráz O, Schins RPF, Chirino YI. Cell type specific cytoskeleton disruption induced by engineered nanoparticles. *Environ Sci Nano*. 2018;5(2):228-245. doi:10.1039/C7EN00704C

50. Maysinger D, Moquin A, Choi J, Kodiha M, Stochaj U. Gold nanourchins and celastrol reorganize the nucleo- and cytoskeleton of glioblastoma cells. *Nanoscale*. 2018;10(4):1716-1726. doi:10.1039/c7nr07833a

51. Mytych J, Pacyk K, Pepek M, Zebrowski J, Lewinska A, Wnuk M. Nanoparticle-mediated decrease of lamin B1 pools promotes a TRF protein-based adaptive response in cultured cells. *Biomaterials*. 2015;53:107-116. doi:10.1016/J.BIOMATERIALS.2015.02.072

52. Hopkins BL, Neumann CA. Redoxins as gatekeepers of the transcriptional oxidative stress response. *Redox Biol*. 2019;21:101104. doi:10.1016/J.REDOX.2019.101104

53. Lingappan K. NF-κB in oxidative stress. *Curr Opin Toxicol*. 2018;7:81-86. doi:10.1016/J.COTOX.2017.11.002

54. Tam AB, Mercado EL, Hoffmann A, Niwa M. ER Stress Activates NF-κB by Integrating Functions of Basal IKK Activity, IRE1 and PERK. *PLoS One*. 2012;7(10):45078. doi:10.1371/JOURNAL.PONE.0045078

55. Cullinan SB, Zhang D, Hannink M, Arvisais E, Kaufman RJ, Diehl JA. Nrf2 is a direct PERK substrate and effector of PERK-dependent cell survival. *Mol Cell Biol*. 2003;23(20):7198-7209. doi:10.1128/MCB.23.20.7198-7209.2003

56. Cullinan SB, Diehl JA. Coordination of ER and oxidative stress signaling: the PERK/Nrf2 signaling pathway. *Int J Biochem Cell Biol*. 2006;38(3):317-332. doi:10.1016/J.BIOCEL.2005.09.018

57. Thoms HC, Stark LA. The NF-κB Nucleolar Stress Response Pathway. *Biomedicines*. 2021;9(9). doi:10.3390/BIOMEDICINES9091082

58. Yang K, Yang J, Yi J. Nucleolar Stress: hallmarks, sensing mechanism and diseases. *Cell Stress*. 2018;2(6):125. doi:10.15698/CST2018.06.139

59. Maehama T, Nishio | Miki, Otani J, Tak |, Mak W, Suzuki A. Nucleolar stress: Molecular mechanisms and related human diseases. *Cancer Sci*. 2023;00:1-9. doi:10.1111/CAS.15755

60. Pfister AS. Emerging role of the nucleolar stress response in autophagy. *Front Cell Neurosci*. 2019;13:444739. doi:10.3389/FNCEL.2019.00156/BIBTEX

61. Chaillou T, Kirby TJ, Mccarthy JJ. Ribosome biogenesis: emerging evidence for a central role in the regulation of skeletal muscle mass. *J Cell Physiol*. 2014;229(11):1584. doi:10.1002/JCP.24604

62. Jayaraj GG, Hipp MS, Ulrich Hartl F. Functional Modules of the Proteostasis Network. *Cold Spring Harb Perspect Biol*. 2020;12(1). doi:10.1101/CSHPERSPECT.A033951

63. Martínez G, Duran-Aniotz C, Cabral-Miranda F, Vivar JP, Hetz C. Endoplasmic reticulum proteostasis impairment in aging. *Aging Cell*. 2017;16(4):615-623. doi:10.1111/ACEL.12599

64. Chu S, Xie X, Payan C, Stochaj U. Valosin containing protein (VCP): initiator, modifier, and potential drug target for neurodegenerative diseases. *Molecular Neurodegeneration 2023 18:1*. 2023;18(1):1-34. doi:10.1186/S13024-023-00639-Y

65. Cao SS, Kaufman RJ. Endoplasmic Reticulum Stress and Oxidative Stress in Cell Fate Decision and Human Disease. *Antioxid Redox Signal*. 2014;21(3):396. doi:10.1089/ARS.2014.5851

66. Greinert R, Volkmer B, Henning S, et al. UVA-induced DNA double-strand breaks result from the repair of clustered oxidative DNA damages. *Nucleic Acids Res*. 2012;40(20):10263-10273. doi:10.1093/NAR/GKS824

67. Podhorecka M, Skladanowski A, Bozko P. H2AX Phosphorylation: Its Role in DNA Damage Response and Cancer Therapy. *J Nucleic Acids*. 2010;2010. doi:10.4061/2010/920161

68. Gruosso T, Mieulet V, Cardon M, et al. Chronic oxidative stress promotes H2AX protein degradation and enhances chemosensitivity in breast cancer patients. *EMBO Mol Med*. 2016;8(5):527-549. doi:10.15252/EMMM.201505891

69. Ding B, Sepehrimanesh M. Nucleocytoplasmic Transport: Regulatory Mechanisms and the Implications in Neurodegeneration. *Int J Mol Sci*. 2021;22(8):4165. doi:10.3390/IJMS22084165

70. Kalita J, Kapinos LE, Zheng T, Rencurel C, Zilman A, Lim RYH. Karyopherin enrichment and compensation fortifies the nuclear pore complex against nucleocytoplasmic leakage. *Journal of Cell Biology*. 2022;221(3). doi:10.1083/JCB.202108107/212986

71. Okada N, Ishigami Y, Suzuki T, et al. Importins and exportins in cellular differentiation. *J Cell Mol Med*. 2008;12(5b):1863. doi:10.1111/J.1582-4934.2008.00437.X

72. Okamura M, Inose H, Masuda S. RNA Export through the NPC in Eukaryotes. *Genes 2015, Vol 6, Pages 124-149*. 2015;6(1):124-149. doi:10.3390/GENES6010124

73. Chung JH, Ryu JH, Lee SY, Kang SH, Shim KB. Effect of Yb3+ and Tm3+ concentrations on blue and NIR upconversion luminescence in Yb3+, Tm3+ co-doped CaMoO4. *Ceram Int*. 2013;39(2):1951-1956. doi:10.1016/j.ceramint.2012.08.045

74. Ho TH, Yang CH, Jiang ZE, Lin HY, Chen YF, Wang TL. NIR-Triggered Generation of Reactive Oxygen Species and Photodynamic Therapy Based on Mesoporous Silica-Coated LiYF4 Upconverting Nanoparticles. *Int J Mol Sci*. 2022;23(15):8757. doi:10.3390/IJMS23158757/S1

75. Tan TT, Selvan ST, Zhao L, Gao S, Ying JY. Size control, shape evolution, and silica coating of near-infrared-emitting PbSe quantum dots. *Chemistry of Materials*.

2007;19(13):3112-3117. doi:10.1021/CM061974E/SUPPL_FILE/CM061974ESI20070220_095102.PDF

76. Ureña-Horno E, Kyriazi ME, Kanaras AG. A method for the growth of uniform silica shells on different size and morphology upconversion nanoparticles. *Nanoscale Adv*. 2021;3(12):3522-3529. doi:10.1039/D0NA00858C

77. Jao CY, Salic A. Exploring RNA transcription and turnover in vivo by using click chemistry. *Proc Natl Acad Sci U S A*. 2008;105(41):15779. doi:10.1073/PNAS.0808480105

78. Fernandes IR, Russo FB, Pignatari GC, et al. Fibroblast sources: Where can we get them? *Cytotechnology*. 2016;68(2):223. doi:10.1007/S10616-014-9771-7

79. Yadav RD, Chaudhary A. Nano–bio surface interactions, cellular internalisation in cancer cells and e-data portals of nanomaterials: A review. *IET Nanobiotechnol*. 2021;15(6):519. doi:10.1049/NBT2.12040

80. Samhadaneh DM, Mandl GA, Han Z, et al. Evaluation of Lanthanide-Doped Upconverting Nanoparticles for in Vitro and in Vivo Applications. *ACS Appl Bio Mater*. 2020;3(7):4358-4369. doi:10.1021/acsabm.0c00381

81. Mandl GA, Vettier F, Tessitore G, et al. Combining Pr 3+-Doped Nanoradiosensitizers and Endogenous Protoporphyrin IX for X-ray-Mediated Photodynamic Therapy of Glioblastoma Cells. *Cite This: ACS Appl Bio Mater*. Published online 2023. doi:10.1021/acsabm.3c00201

82. Maluchenko N V., Feofanov A V., Studitsky VM. PARP-1-Associated Pathological Processes: Inhibition by Natural Polyphenols. *Int J Mol Sci*. 2021;22(21). doi:10.3390/IJMS222111441

83. Zhang H, Zhou L, Yuen J, et al. Delayed Nrf2-regulated antioxidant gene induction in response to silica nanoparticles. *Free Radic Biol Med*. 2017;108:311-319. doi:10.1016/J.FREERADBIOMED.2017.04.002

84. Lazarev VF, Nikotina AD, Semenyuk PI, et al. Small molecules preventing GAPDH aggregation are therapeutically applicable in cell and rat models of oxidative stress. *Free Radic Biol Med*. 2016;92:29-38. doi:10.1016/J.FREERADBIOMED.2015.12.025

85. Peltonen K, Colis L, Liu H, et al. A Targeting Modality for Destruction of RNA Polymerase I that Possesses Anticancer Activity. *Cancer Cell*. 2014;25(1):77. doi:10.1016/J.CCR.2013.12.009

86. Guillen-Chable F, Corona UR, Pereira-Santana A, et al. Fibrillarin Ribonuclease Activity is Dependent on the GAR Domain and Modulated by Phospholipids. *Cells*. 2020;9(5). doi:10.3390/CELLS9051143

87. Abdelmohsen K, Gorospe M. RNA-binding protein nucleolin in disease. *RNA Biol*. 2012;9(6):799. doi:10.4161/RNA.19718

88. Brewer JW, Hendershot LM, Sherr CJ, Diehl JA. Mammalian unfolded protein response inhibits cyclin D1 translation and cell-cycle progression. *Proc Natl Acad Sci U S A*. 1999;96(15):8505. doi:10.1073/PNAS.96.15.8505

89. Poon IKH, Jans DA. Regulation of Nuclear Transport: Central Role in Development and Transformation? *Traffic*. 2005;6(3):173-186. doi:10.1111/J.1600-0854.2005.00268.X

90. Ding B, Sepehrimanesh M. Nucleocytoplasmic Transport: Regulatory Mechanisms and the Implications in Neurodegeneration. *Int J Mol Sci*. 2021;22(8):4165. doi:10.3390/IJMS22084165

91. Exposure to the metabolic inhibitor sodium azide induces stress protein expression and thermotolerance in the nematode Caenorhabditis elegans - PubMed. Accessed November 9, 2023. https://pubmed.ncbi.nlm.nih.gov/12820649/

92. Oka M, Asally M, Yasuda Y, Ogawa Y, Tachibana T, Yoneda Y. The Mobile FG Nucleoporin Nup98 Is a Cofactor for Crm1-dependent Protein Export. *Mol Biol Cell*. 2010;21(11):1885. doi:10.1091/MBC.E09-12-1041

93. Souquere S, Weil D, Pierron G. Comparative ultrastructure of CRM1-Nucleolar bodies (CNoBs), Intranucleolar bodies (INBs) and hybrid PML/p62 bodies uncovers new facets of nuclear body dynamic and diversity. *Nucleus*. 2015;6(4):326. doi:10.1080/19491034.2015.1082695

94. Bai B, Moore HM, Laiho M. CRM1 and its ribosome export adaptor NMD3 localize to the nucleolus and affect rRNA synthesis. *Nucleus (United States)*. 2013;4(4):315-325. doi:10.4161/NUCL.25342/SUPPL_FILE/KNCL_A_10925342_SM0001.ZIP

95. Yeyeodu ST, Martin ME, Reaves DK, Enders JR, Costantini LM, Fleming JM. Experimental data demonstrating the effects of silver nanoparticles on basement membrane gene and protein expression in cultured colon, mammary and bronchial epithelia. *Data Brief*. 2019;26:104464. doi:10.1016/J.DIB.2019.104464

96. Martin ME, Reaves DK, Jeffcoat B, et al. Silver nanoparticles alter epithelial basement membrane integrity, cell adhesion molecule expression, and TGF-β1 secretion. *Nanomedicine*. 2019;21:102070. doi:10.1016/J.NANO.2019.102070

97. Tsai TL, Hou CC, Wang HC, et al. Nucleocytoplasmic transport blockage by SV40 peptide-modified gold nanoparticles induces cellular autophagy. *Int J Nanomedicine*. 2012;7:5215-5234. doi:10.2147/IJN.S35125

98. Shukla RK, Badiye A, Vajpayee K, Kapoor N. Genotoxic Potential of Nanoparticles: Structural and Functional Modifications in DNA. *Front Genet*. 2021;12. doi:10.3389/FGENE.2021.728250

99. Lesbirel S, Wilson SA. The m6A-methylase complex and mRNA export. *Biochim Biophys Acta Gene Regul Mech*. 2019;1862(3):319. doi:10.1016/J.BBAGRM.2018.09.008

100. Zhang M, Song J, Yuan W, Zhang W, Sun Z. Roles of RNA Methylation on Tumor Immunity and Clinical Implications. *Front Immunol*. 2021;12:641507. doi:10.3389/FIMMU.2021.641507/BIBTEX

101. Lesbirel S, Wilson SA. The m6A-methylase complex and mRNA export. *Biochim Biophys Acta Gene Regul Mech*. 2019;1862(3):319. doi:10.1016/J.BBAGRM.2018.09.008

102. Wang Y, Ruan F, Zuo Z, He C. Nanoparticle-Induced m6A RNA Modification: Detection Methods, Mechanisms and Applications. *Nanomaterials*. 2022;12(3):12. doi:10.3390/NANO12030389

JOHN WILEY AND SONS LICENSE
TERMS AND CONDITIONS

Oct 26, 2023

This Agreement between Mr. Kais Bietar ("You") and John Wiley and Sons ("John Wiley and Sons") consists of your license details and the terms and conditions provided by John Wiley and Sons and Copyright Clearance Center.

License Number	5656700822307
License date	Oct 26, 2023
Licensed Content Publisher	John Wiley and Sons
Licensed Content Publication	Journal of Cellular and Molecular Medicine
Licensed Content Title	Importins and exportins in cellular differentiation
Licensed Content Author	Norihisa Okada, Yoko Ishigami, Takuji Suzuki, et al
Licensed Content Date	Oct 30, 2008
Licensed Content Volume	12
Licensed Content Issue	5b
Licensed Content Pages	9
Type of use	Dissertation/Thesis
Requestor type	University/Academic

Format	Electronic
Portion	Figure/table
Number of figures/tables	1
Will you be translating?	No
Title of new work	Assessing the effects of lanthanide-doped upconverting nanoparticles on the cellular homeostasis of healthy mammalian cells
Institution name	McGill University
Expected presentation date	Dec 2023
Portions	Figure 1
Requestor Location	Mr. Kais Bietar 3655 Promenade Sir William Osler Montreal, QC H3A 1A3 Canada Attn: Mcgill university
Publisher Tax ID	EU826007151
Total	0.00 USD

Terms and Conditions

TERMS AND CONDITIONS

This copyrighted material is owned by or exclusively licensed to John Wiley & Sons, Inc. or one of its group companies (each a"Wiley Company") or handled on behalf of a society with which a Wiley Company has exclusive publishing rights in relation to a particular

work (collectively "WILEY"). By clicking "accept" in connection with completing this licensing transaction, you agree that the following terms and conditions apply to this transaction (along with the billing and payment terms and conditions established by the Copyright Clearance Center Inc., ("CCC's Billing and Payment terms and conditions"), at the time that you opened your RightsLink account (these are available at any time at http://myaccount.copyright.com).

Terms and Conditions

- The materials you have requested permission to reproduce or reuse (the "Wiley Materials") are protected by copyright.
- You are hereby granted a personal, non-exclusive, non-sub licensable (on a stand-alone basis), non-transferable, worldwide, limited license to reproduce the Wiley Materials for the purpose specified in the licensing process. This license, **and any CONTENT (PDF or image file) purchased as part of your order,** is for a one-time use only and limited to any maximum distribution number specified in the license. The first instance of republication or reuse granted by this license must be completed within two years of the date of the grant of this license (although copies prepared before the end date may be distributed thereafter). The Wiley Materials shall not be used in any other manner or for any other purpose, beyond what is granted in the license. Permission is granted subject to an appropriate acknowledgement given to the author, title of the material/book/journal and the publisher. You shall also duplicate the copyright notice that appears in the Wiley publication in your use of the Wiley Material. Permission is also granted on the understanding that nowhere in the text is a previously published source acknowledged for all or part of this Wiley Material. Any third party content is expressly excluded from this permission.
- With respect to the Wiley Materials, all rights are reserved. Except as expressly granted by the terms of the license, no part of the Wiley Materials may be copied, modified, adapted (except for minor reformatting required by the new Publication), translated, reproduced, transferred or distributed, in any form or by any means, and no derivative works may be made based on the Wiley Materials without the prior permission of the respective copyright owner.**For STM Signatory Publishers clearing permission under the terms of the STM Permissions Guidelines only, the terms of the license are extended to include subsequent editions and for editions in other languages, provided such editions are for the work as a whole in situ and does not involve the separate exploitation of the permitted figures or extracts,** You may not alter, remove or suppress in any manner any copyright, trademark or other notices displayed by the Wiley Materials. You may not license, rent, sell, loan, lease, pledge, offer as security, transfer or assign the Wiley Materials on a stand-alone basis, or any of the rights granted to you hereunder to any other person.
- The Wiley Materials and all of the intellectual property rights therein shall at all times remain the exclusive property of John Wiley & Sons Inc, the Wiley Companies, or their respective licensors, and your interest therein is only that of having possession of and the right to reproduce the Wiley Materials pursuant to Section 2 herein during the continuance of this Agreement. You agree that you own no right, title or interest in or to the Wiley Materials or any of the intellectual property rights therein. You shall have no rights hereunder other than the license as provided for above in Section 2. No right, license or interest to any trademark, trade

name, service mark or other branding ("Marks") of WILEY or its licensors is granted hereunder, and you agree that you shall not assert any such right, license or interest with respect thereto

- NEITHER WILEY NOR ITS LICENSORS MAKES ANY WARRANTY OR REPRESENTATION OF ANY KIND TO YOU OR ANY THIRD PARTY, EXPRESS, IMPLIED OR STATUTORY, WITH RESPECT TO THE MATERIALS OR THE ACCURACY OF ANY INFORMATION CONTAINED IN THE MATERIALS, INCLUDING, WITHOUT LIMITATION, ANY IMPLIED WARRANTY OF MERCHANTABILITY, ACCURACY, SATISFACTORY QUALITY, FITNESS FOR A PARTICULAR PURPOSE, USABILITY, INTEGRATION OR NON-INFRINGEMENT AND ALL SUCH WARRANTIES ARE HEREBY EXCLUDED BY WILEY AND ITS LICENSORS AND WAIVED BY YOU.

- WILEY shall have the right to terminate this Agreement immediately upon breach of this Agreement by you.

- You shall indemnify, defend and hold harmless WILEY, its Licensors and their respective directors, officers, agents and employees, from and against any actual or threatened claims, demands, causes of action or proceedings arising from any breach of this Agreement by you.

- IN NO EVENT SHALL WILEY OR ITS LICENSORS BE LIABLE TO YOU OR ANY OTHER PARTY OR ANY OTHER PERSON OR ENTITY FOR ANY SPECIAL, CONSEQUENTIAL, INCIDENTAL, INDIRECT, EXEMPLARY OR PUNITIVE DAMAGES, HOWEVER CAUSED, ARISING OUT OF OR IN CONNECTION WITH THE DOWNLOADING, PROVISIONING, VIEWING OR USE OF THE MATERIALS REGARDLESS OF THE FORM OF ACTION, WHETHER FOR BREACH OF CONTRACT, BREACH OF WARRANTY, TORT, NEGLIGENCE, INFRINGEMENT OR OTHERWISE (INCLUDING, WITHOUT LIMITATION, DAMAGES BASED ON LOSS OF PROFITS, DATA, FILES, USE, BUSINESS OPPORTUNITY OR CLAIMS OF THIRD PARTIES), AND WHETHER OR NOT THE PARTY HAS BEEN ADVISED OF THE POSSIBILITY OF SUCH DAMAGES. THIS LIMITATION SHALL APPLY NOTWITHSTANDING ANY FAILURE OF ESSENTIAL PURPOSE OF ANY LIMITED REMEDY PROVIDED HEREIN.

- Should any provision of this Agreement be held by a court of competent jurisdiction to be illegal, invalid, or unenforceable, that provision shall be deemed amended to achieve as nearly as possible the same economic effect as the original provision, and the legality, validity and enforceability of the remaining provisions of this Agreement shall not be affected or impaired thereby.

- The failure of either party to enforce any term or condition of this Agreement shall not constitute a waiver of either party's right to enforce each and every term and condition of this Agreement. No breach under this agreement shall be deemed waived or excused by either party unless such waiver or consent is in writing signed by the party granting such waiver or consent. The waiver by or consent of a party to a breach of any provision of this Agreement shall not operate or be construed as a waiver of or consent to any other or subsequent breach by such other party.

- This Agreement may not be assigned (including by operation of law or otherwise) by you without WILEY's prior written consent.

- Any fee required for this permission shall be non-refundable after thirty (30) days from receipt by the CCC.
- These terms and conditions together with CCC's Billing and Payment terms and conditions (which are incorporated herein) form the entire agreement between you and WILEY concerning this licensing transaction and (in the absence of fraud) supersedes all prior agreements and representations of the parties, oral or written. This Agreement may not be amended except in writing signed by both parties. This Agreement shall be binding upon and inure to the benefit of the parties' successors, legal representatives, and authorized assigns.
- In the event of any conflict between your obligations established by these terms and conditions and those established by CCC's Billing and Payment terms and conditions, these terms and conditions shall prevail.
- WILEY expressly reserves all rights not specifically granted in the combination of (i) the license details provided by you and accepted in the course of this licensing transaction, (ii) these terms and conditions and (iii) CCC's Billing and Payment terms and conditions.
- This Agreement will be void if the Type of Use, Format, Circulation, or Requestor Type was misrepresented during the licensing process.
- This Agreement shall be governed by and construed in accordance with the laws of the State of New York, USA, without regards to such state's conflict of law rules. Any legal action, suit or proceeding arising out of or relating to these Terms and Conditions or the breach thereof shall be instituted in a court of competent jurisdiction in New York County in the State of New York in the United States of America and each party hereby consents and submits to the personal jurisdiction of such court, waives any objection to venue in such court and consents to service of process by registered or certified mail, return receipt requested, at the last known address of such party.

WILEY OPEN ACCESS TERMS AND CONDITIONS

Wiley Publishes Open Access Articles in fully Open Access Journals and in Subscription journals offering Online Open. Although most of the fully Open Access journals publish open access articles under the terms of the Creative Commons Attribution (CC BY) License only, the subscription journals and a few of the Open Access Journals offer a choice of Creative Commons Licenses. The license type is clearly identified on the article.

The Creative Commons Attribution License

The Creative Commons Attribution License (CC-BY) allows users to copy, distribute and transmit an article, adapt the article and make commercial use of the article. The CC-BY license permits commercial and non-

Creative Commons Attribution Non-Commercial License

The Creative Commons Attribution Non-Commercial (CC-BY-NC)License permits use, distribution and reproduction in any medium, provided the original work is properly cited and is not used for commercial purposes.(see below)

Creative Commons Attribution-Non-Commercial-NoDerivs License

The Creative Commons Attribution Non-Commercial-NoDerivs License (CC-BY-NC-ND) permits use, distribution and reproduction in any medium, provided the original work is properly cited, is not used for commercial purposes and no modifications or adaptations are made. (see below)

Use by commercial "for-profit" organizations

Use of Wiley Open Access articles for commercial, promotional, or marketing purposes requires further explicit permission from Wiley and will be subject to a fee.

Further details can be found on Wiley Online Library
http://olabout.wiley.com/WileyCDA/Section/id-410895.html

Other Terms and Conditions:

v1.10 Last updated September 2015

Questions? customercare@copyright.com.

SPRINGER NATURE LICENSE
TERMS AND CONDITIONS

Oct 26, 2023

This Agreement between Mr. Kais Bietar ("You") and Springer Nature ("Springer Nature") consists of your license details and the terms and conditions provided by Springer Nature and Copyright Clearance Center.

License Number	5656650829535
License date	Oct 26, 2023
Licensed Content Publisher	Springer Nature
Licensed Content Publication	Nature Reviews Drug Discovery
Licensed Content Title	Engineering precision nanoparticles for drug delivery
Licensed Content Author	Michael J. Mitchell et al
Licensed Content Date	Dec 4, 2020
Type of Use	Thesis/Dissertation
Requestor type	academic/university or research institute
Format	electronic
Portion	figures/tables/illustrations
Number of figures/tables/illustrations	1
Would you like a high resolution image with your order?	no

Will you be translating?	no
Circulation/distribution	1 - 29
Author of this Springer Nature content	no
Title of new work	Assessing the effects of lanthanide-doped upconverting nanoparticles on the cellular homeostasis of healthy mammalian cells
Institution name	McGill University
Expected presentation date	Dec 2023
Portions	Figure 5
Requestor Location	Mr. Kais Bietar 3655 Promenade Sir William Osler Montreal, QC H3A 1A3 Canada Attn: McGill University
Total	0.00 USD

Terms and Conditions

Springer Nature Customer Service Centre GmbH Terms and Conditions

The following terms and conditions ("Terms and Conditions") together with the terms specified in your [RightsLink] constitute the License ("License") between you as Licensee and Springer Nature Customer Service Centre GmbH as Licensor. By clicking 'accept' and completing the transaction for your use of the material ("Licensed Material"), you confirm your acceptance of and obligation to be bound by these Terms and Conditions.

1. Grant and Scope of License

1. 1. The Licensor grants you a personal, non-exclusive, non-transferable, non-sublicensable, revocable, world-wide License to reproduce, distribute, communicate to the public, make available, broadcast, electronically transmit or create derivative

works using the Licensed Material for the purpose(s) specified in your RightsLink Licence Details only. Licenses are granted for the specific use requested in the order and for no other use, subject to these Terms and Conditions. You acknowledge and agree that the rights granted to you under this License do not include the right to modify, edit, translate, include in collective works, or create derivative works of the Licensed Material in whole or in part unless expressly stated in your RightsLink Licence Details. You may use the Licensed Material only as permitted under this Agreement and will not reproduce, distribute, display, perform, or otherwise use or exploit any Licensed Material in any way, in whole or in part, except as expressly permitted by this License.

1. 2. You may only use the Licensed Content in the manner and to the extent permitted by these Terms and Conditions, by your RightsLink Licence Details and by any applicable laws.

1. 3. A separate license may be required for any additional use of the Licensed Material, e.g. where a license has been purchased for print use only, separate permission must be obtained for electronic re-use. Similarly, a License is only valid in the language selected and does not apply for editions in other languages unless additional translation rights have been granted separately in the License.

1. 4. Any content within the Licensed Material that is owned by third parties is expressly excluded from the License.

1. 5. Rights for additional reuses such as custom editions, computer/mobile applications, film or TV reuses and/or any other derivative rights requests require additional permission and may be subject to an additional fee. Please apply to journalpermissions@springernature.com or bookpermissions@springernature.com for these rights.

2. Reservation of Rights

Licensor reserves all rights not expressly granted to you under this License. You acknowledge and agree that nothing in this License limits or restricts Licensor's rights in or use of the Licensed Material in any way. Neither this License, nor any act, omission, or statement by Licensor or you, conveys any ownership right to you in any Licensed Material, or to any element or portion thereof. As between Licensor and you, Licensor owns and retains all right, title, and interest in and to the Licensed Material subject to the license granted in Section 1.1. Your permission to use the Licensed Material is expressly conditioned on you not impairing Licensor's or the applicable copyright owner's rights in the Licensed Material in any way.

3. Restrictions on use

3. 1. Minor editing privileges are allowed for adaptations for stylistic purposes or formatting purposes provided such alterations do not alter the original meaning or intention of the Licensed Material and the new figure(s) are still accurate and representative of the Licensed Material. Any other changes including but not limited to, cropping, adapting, and/or omitting material that affect the meaning, intention or moral rights of the author(s) are strictly prohibited.

3. 2. You must not use any Licensed Material as part of any design or trademark.

3. 3. Licensed Material may be used in Open Access Publications (OAP), but any such reuse must include a clear acknowledgment of this permission visible at the same time as the figures/tables/illustration or abstract and which must indicate that the Licensed Material is not part of the governing OA license but has been reproduced with permission. This may be indicated according to any standard referencing system but must include at a minimum 'Book/Journal title, Author, Journal Name (if applicable), Volume (if applicable), Publisher, Year, reproduced with permission from SNCSC'.

4. STM Permission Guidelines

4. 1. An alternative scope of license may apply to signatories of the STM Permissions Guidelines ("STM PG") as amended from time to time and made available at https://www.stm-assoc.org/intellectual-property/permissions/permissions-guidelines/.

4. 2. For content reuse requests that qualify for permission under the STM PG, and which may be updated from time to time, the STM PG supersede the terms and conditions contained in this License.

4. 3. If a License has been granted under the STM PG, but the STM PG no longer apply at the time of publication, further permission must be sought from the Rightsholder. Contact journalpermissions@springernature.com or bookpermissions@springernature.com for these rights.

5. Duration of License

5. 1. Unless otherwise indicated on your License, a License is valid from the date of purchase ("License Date") until the end of the relevant period in the below table:

Reuse in a medical communications project	Reuse up to distribution or time period indicated in License
Reuse in a dissertation/thesis	Lifetime of thesis
Reuse in a journal/magazine	Lifetime of journal/magazine
Reuse in a book/textbook	Lifetime of edition
Reuse on a website	1 year unless otherwise specified in the License
Reuse in a presentation/slide kit/poster	Lifetime of presentation/slide kit/poster. Note: publication whether electronic or in print of presentation/slide kit/poster may require further permission.
Reuse in conference proceedings	Lifetime of conference proceedings
Reuse in an annual report	Lifetime of annual report
Reuse in training/CME materials	Reuse up to distribution or time period indicated in License
Reuse in newsmedia	Lifetime of newsmedia
Reuse in coursepack/classroom materials	Reuse up to distribution and/or time period indicated in license

6. Acknowledgement

6. 1. The Licensor's permission must be acknowledged next to the Licensed Material in print. In electronic form, this acknowledgement must be visible at the same time as the figures/tables/illustrations or abstract and must be hyperlinked to the journal/book's homepage.

6. 2. Acknowledgement may be provided according to any standard referencing system and at a minimum should include "Author, Article/Book Title, Journal name/Book imprint, volume, page number, year, Springer Nature".

7. Reuse in a dissertation or thesis

7. 1. Where 'reuse in a dissertation/thesis' has been selected, the following terms apply: Print rights of the Version of Record are provided for; electronic rights for use only on institutional repository as defined by the Sherpa guideline (www.sherpa.ac.uk/romeo/) and only up to what is required by the awarding institution.

7. 2. For theses published under an ISBN or ISSN, separate permission is required. Please contact journalpermissions@springernature.com or bookpermissions@springernature.com for these rights.

7. 3. Authors must properly cite the published manuscript in their thesis according to current citation standards and include the following acknowledgement: '*Reproduced with permission from Springer Nature*'.

8. License Fee

You must pay the fee set forth in the License Agreement (the "License Fees"). All amounts payable by you under this License are exclusive of any sales, use, withholding, value added or similar taxes, government fees or levies or other assessments. Collection and/or remittance of such taxes to the relevant tax authority shall be the responsibility of the party who has the legal obligation to do so.

9. Warranty

9. 1. The Licensor warrants that it has, to the best of its knowledge, the rights to license reuse of the Licensed Material. **You are solely responsible for ensuring that the material you wish to license is original to the Licensor and does not carry the copyright of another entity or third party (as credited in the published version).** If the credit line on any part of the Licensed Material indicates that it was reprinted or adapted with permission from another source, then you should seek additional permission from that source to reuse the material.

9. 2. EXCEPT FOR THE EXPRESS WARRANTY STATED HEREIN AND TO THE EXTENT PERMITTED BY APPLICABLE LAW, LICENSOR PROVIDES THE LICENSED MATERIAL "AS IS" AND MAKES NO OTHER REPRESENTATION OR WARRANTY. LICENSOR EXPRESSLY DISCLAIMS ANY LIABILITY FOR ANY CLAIM ARISING FROM OR OUT OF THE CONTENT, INCLUDING BUT NOT LIMITED TO ANY ERRORS, INACCURACIES, OMISSIONS, OR DEFECTS CONTAINED THEREIN, AND ANY IMPLIED OR EXPRESS WARRANTY AS TO MERCHANTABILITY OR FITNESS FOR A PARTICULAR PURPOSE. IN NO EVENT SHALL LICENSOR

BE LIABLE TO YOU OR ANY OTHER PARTY OR ANY OTHER PERSON OR FOR ANY SPECIAL, CONSEQUENTIAL, INCIDENTAL, INDIRECT, PUNITIVE, OR EXEMPLARY DAMAGES, HOWEVER CAUSED, ARISING OUT OF OR IN CONNECTION WITH THE DOWNLOADING, VIEWING OR USE OF THE LICENSED MATERIAL REGARDLESS OF THE FORM OF ACTION, WHETHER FOR BREACH OF CONTRACT, BREACH OF WARRANTY, TORT, NEGLIGENCE, INFRINGEMENT OR OTHERWISE (INCLUDING, WITHOUT LIMITATION, DAMAGES BASED ON LOSS OF PROFITS, DATA, FILES, USE, BUSINESS OPPORTUNITY OR CLAIMS OF THIRD PARTIES), AND WHETHER OR NOT THE PARTY HAS BEEN ADVISED OF THE POSSIBILITY OF SUCH DAMAGES. THIS LIMITATION APPLIES NOTWITHSTANDING ANY FAILURE OF ESSENTIAL PURPOSE OF ANY LIMITED REMEDY PROVIDED HEREIN.

10. Termination and Cancellation

10. 1. The License and all rights granted hereunder will continue until the end of the applicable period shown in Clause 5.1 above. Thereafter, this license will be terminated and all rights granted hereunder will cease.

10. 2. Licensor reserves the right to terminate the License in the event that payment is not received in full or if you breach the terms of this License.

11. General

11. 1. The License and the rights and obligations of the parties hereto shall be construed, interpreted and determined in accordance with the laws of the Federal Republic of Germany without reference to the stipulations of the CISG (United Nations Convention on Contracts for the International Sale of Goods) or to Germany´s choice-of-law principle.

11. 2. The parties acknowledge and agree that any controversies and disputes arising out of this License shall be decided exclusively by the courts of or having jurisdiction for Heidelberg, Germany, as far as legally permissible.

11. 3. This License is solely for Licensor's and Licensee's benefit. It is not for the benefit of any other person or entity.

Questions? For questions on Copyright Clearance Center accounts or website issues please contact springernaturesupport@copyright.com or +1-855-239-3415 (toll free in the US) or +1-978-646-2777. For questions on Springer Nature licensing please visit https://www.springernature.com/gp/partners/rights-permissions-third-party-distribution

Other Conditions:

Version 1.4 - Dec 2022

Questions? customercare@copyright.com.

Marketplace

Order Confirmation

Thank you, your order has been placed. An email confirmation has been sent to you. Your order license details and printable licenses will be available within 24 hours. Please access Manage Account for final order details.

This is not an invoice. Please go to manage account to access your order history and invoices.

CUSTOMER INFORMATION

Payment by invoice: You can cancel your order until the invoice is generated by contacting customer service.

Billing Address

Mr. Kais Bietar
3655 Promenade Sir William Osler
Montreal, QC H3A 1A3
Canada

+1 4387738262
kais.bietar@mail.mcgill.ca

Customer Location

Mr. Kais Bietar
3655 Promenade Sir William Osler
Montreal, QC H3A 1A3
Canada

PO Number (optional)

N/A

Payment options

Invoice

PENDING ORDER CONFIRMATION

Confirmation Number: Pending

Order Date: 26-Oct-2023

1. Materials Chemistry Frontiers

0.00 USD

Article: Synthesis and Fundamental Studies of a Photoresponsive Oligonucleotide-Upconverting Nanoparticle Covalent Conjugate

Order License ID	Pending	**Publisher**	Royal Society of Chemistry
ISSN	2052-1537		
Type of Use	Republish in a thesis/dissertation	**Portion**	Chart/graph/table/figure

LICENSED CONTENT

Publication Title	Materials Chemistry Frontiers	**Rightsholder**	Royal Society of Chemistry
Article Title	Synthesis and Fundamental Studies of a Photoresponsive Oligonucleotide-Upconverting Nanoparticle Covalent Conjugate	**Publication Type**	e-Journal
		Start Page	4690
		End Page	4699
		Issue	12
Author/Editor	Zhongguo hua xue hui (Beijing, China), Royal Society of Chemistry (Great Britain)	**Volume**	5
Date	01/01/2016		

Language	English
Country	United Kingdom of Great Britain and Northern Ireland

REQUEST DETAILS

Portion Type	Chart/graph/table/figure	Distribution	Worldwide
Number of Charts / Graphs / Tables / Figures Requested	3	Translation	Original language of publication
Format (select all that apply)	Electronic	Copies for the Disabled?	No
Who Will Republish the Content?	Academic institution	Minor Editing Privileges?	Yes
		Incidental Promotional Use?	No
Duration of Use	Life of current edition	Currency	USD
Lifetime Unit Quantity	Up to 499		
Rights Requested	Main product		

NEW WORK DETAILS

Title	Assessing the effects of lanthanide-doped upconverting nanoparticles on the cellular homeostasis of healthy mammalian cells	Institution Name	McGill University
		Expected Presentation Date	2023-12-15
Instructor Name	Dr. Ursula Stochaj		

ADDITIONAL DETAILS

Order Reference Number	N/A	The Requesting Person / Organization to Appear on the License	Kais Bietar

REQUESTED CONTENT DETAILS

Title, Description or Numeric Reference of the Portion(s)	Figure 1, Figure 3 and Figure 4	Title of the Article / Chapter the Portion Is From	Synthesis and Fundamental Studies of a Photoresponsive Oligonucleotide-Upconverting Nanoparticle Covalent Conjugate
Editor of Portion(s)	Liczner, Christopher; Mandl, Gabrielle A.; Maurizio, Steven L.; Duke, Kieran; Capobianco, John A.; Wilds, Christopher James	Author of Portion(s)	Liczner, Christopher; Mandl, Gabrielle A.; Maurizio, Steven L.; Duke, Kieran; Capobianco, John A.; Wilds, Christopher James
Volume / Edition	5		
Page or Page Range of Portion	4690-4699	Issue, if Republishing an Article From a Serial	12
		Publication Date of Portion	2021-01-01

Total Items: 1

Total Due: 0.00 USD

Accepted: Marketplace Permissions General Terms and Conditions and any applicable Publisher Terms and Conditions